Frequency-difference Electrical Impedance Tomography

Jeehyun Lee[1], Jin Keun Seo[1], Eung Je Woo[2], and David Holder[3]

[1]Department of Computational Science and Engineering, Yonsei University, Seoul, Korea

[2]College of Electronics and Information, Kyung Hee University, Korea

[3]Department of Medical Physics, University College London, London, UK

San Jose State University, October 6th 2010

Electrical Impedance Tomography

Computerized tomography (CT)

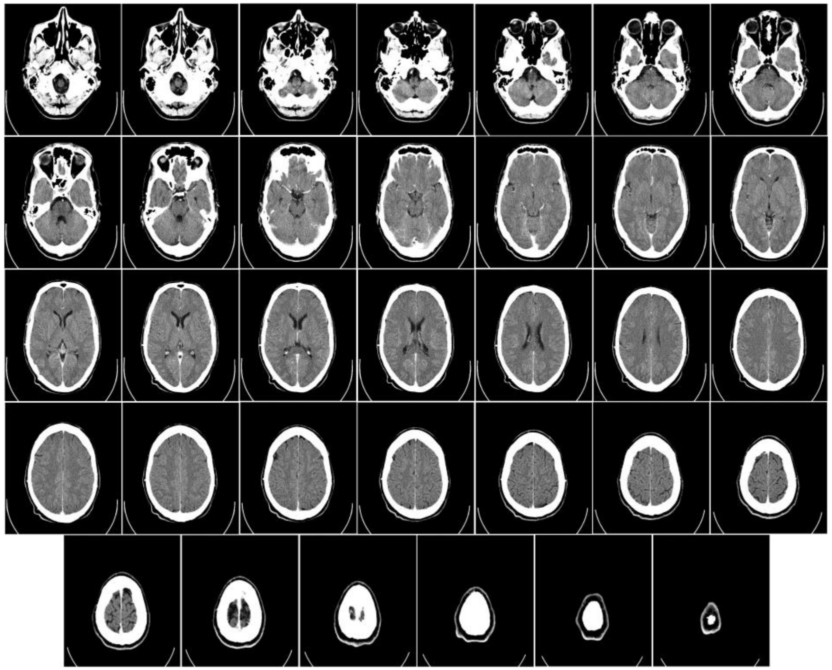

Magnetic resonance imaging (MRI)

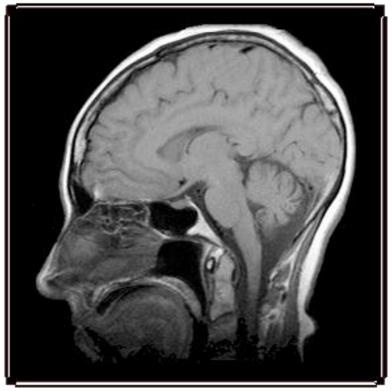

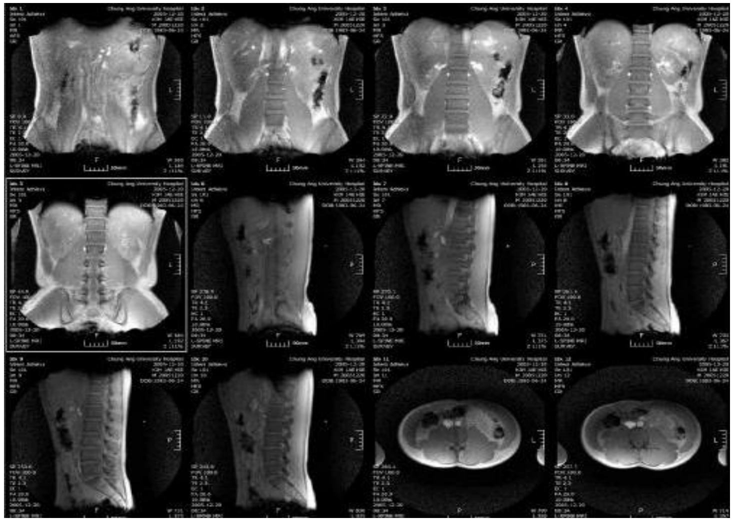

Electrical Impedance Tomography

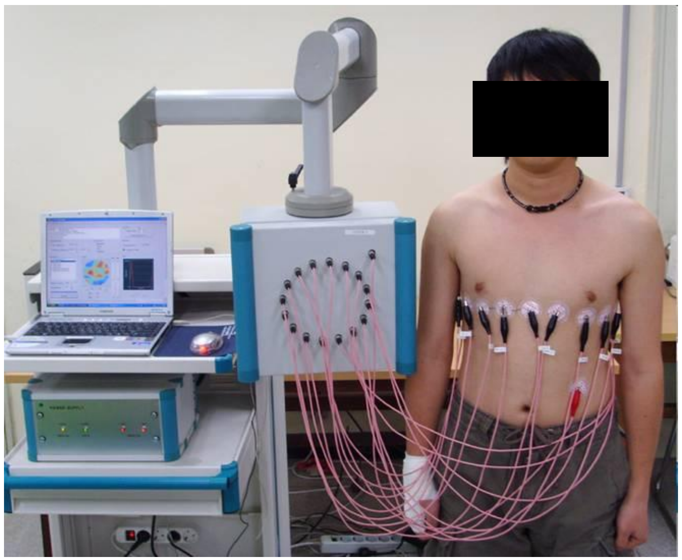

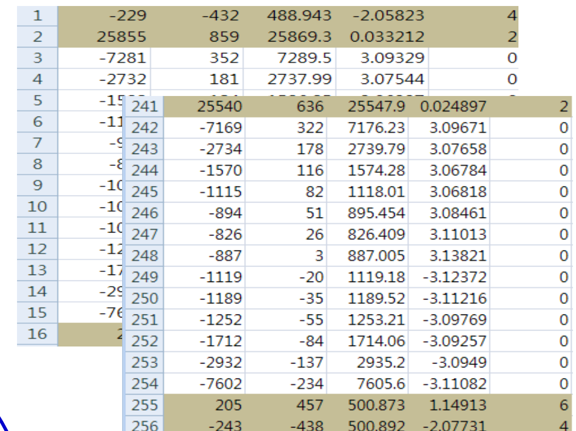

1	-229	-432	488.943	-2.05823	4
2	25855	859	25869.3	0.033212	2
3	-7281	352	7289.5	3.09329	0
4	-2732	181	2737.99	3.07544	0
5	-15				
6	-11				
7	-9				
8	-8				
9	-10				
10	-10				
11	-10				
12	-12				
13	-17				
14	-29				
15	-76				
16	2				

241	25540	636	25547.9	0.024897	2
242	-7169	322	7176.23	3.09671	0
243	-2734	178	2739.79	3.07658	0
244	-1570	116	1574.28	3.06784	0
245	-1115	82	1118.01	3.06818	0
246	-894	51	895.454	3.08461	0
247	-826	26	826.409	3.11013	0
248	-887	3	887.005	3.13821	0
249	-1119	-20	1119.18	-3.12372	0
250	-1189	-35	1189.52	-3.11216	0
251	-1252	-55	1253.21	-3.09769	0
252	-1712	-84	1714.06	-3.09257	0
253	-2932	-137	2935.2	-3.0949	0
254	-7602	-234	7605.6	-3.11082	0
255	205	457	500.873	1.14913	6
256	-243	-438	500.892	-2.07731	4

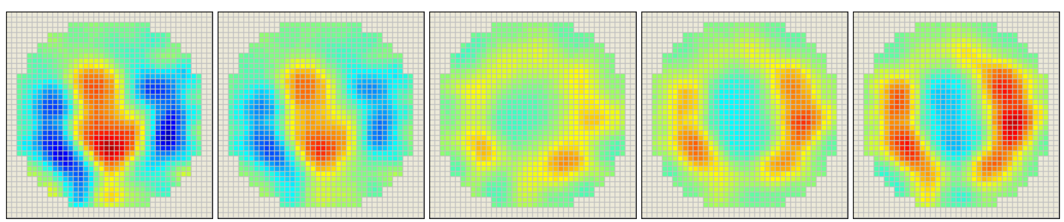

Inhale ⟷ Exhale

Electrical Impedance Tomography

Viewing the human subject as a mixture of resistance and reactance, we can evaluate electrical properties of the subject by injecting a sinusoidal current between two electrodes attached on the surface boundary of the subject and measuring the voltage drop at the surface. EIT is based on this bio-impedance techniques.

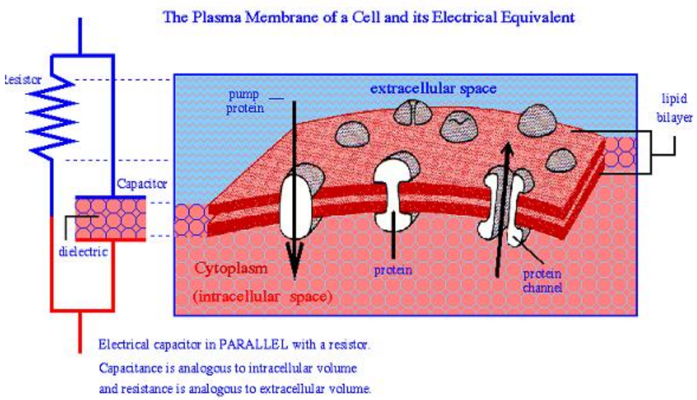

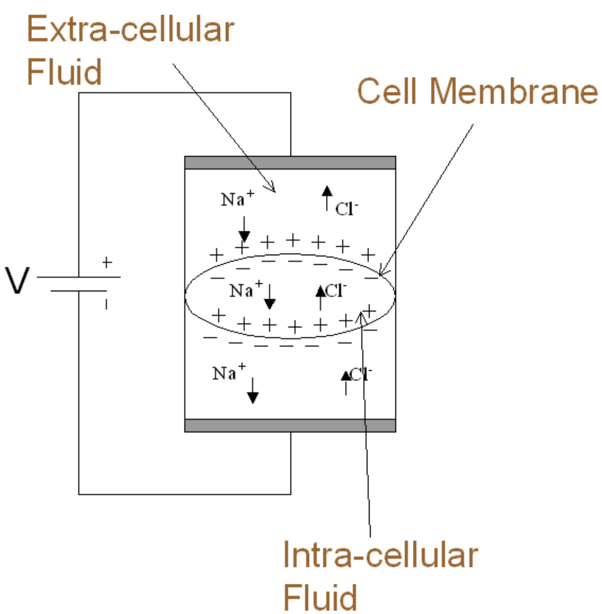

What is Electrical Impedance Tomography?

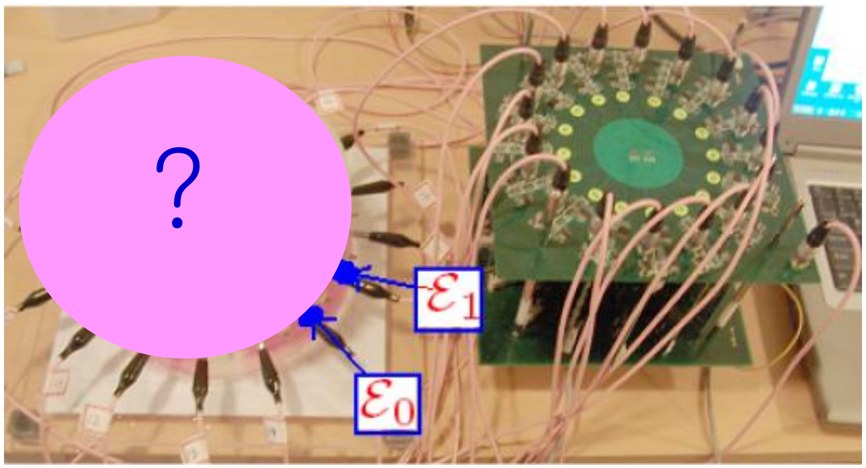

conductivity
reconstruction

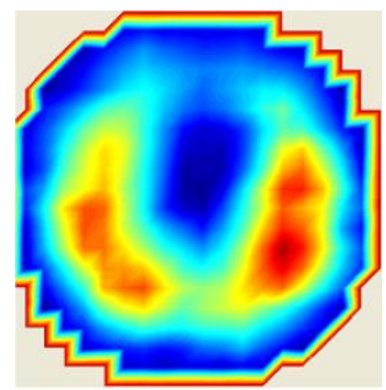

inject current through surface electrodes

measure boundary voltage data

reconstruct images of conductivity distribution

complex conductivity $\gamma = \sigma + i\omega\epsilon$

Applications

Medical Imaging

Monitoring of pulmonary function

Imaging gastric emptying

Breast cancer detection

Neuroimaging in acute stroke

Geophysics

Information about rock porosity, fracture formation.

Imaging underground conducting fluid plumes for environmental cleaning.

Non destructive testing

Identification of defects (voids, cracks) and corrosion in materials

Tissue	**Resistivity [Ohm/m]**
Cerebrospinal fluid	0.65
Blood	1.5
Liver	3.5
Lung (expiration-inspiration)	7.27-23.63
Fat	20.6
Bone	16.6

Barber and Brown [1984]

Governing Equation in 3-D

Time harmonic electric and magnetic fields at frequency ω,

$$\mathcal{E} = \Re\{\mathbf{E}e^{i\omega t}\}, \quad \mathcal{H} = \Re\{\mathbf{H}e^{i\omega t}\}$$

Maxwell equations give

$$\begin{aligned} \nabla \times \mathbf{H} &= [\sigma + i\,\omega\,\epsilon]\,\mathbf{E} \\ \nabla \times \mathbf{E} &= -i\omega\mu\mathbf{H} \quad \approx \quad 0 \end{aligned}$$

The electric potential u satisfies $\mathbf{E} = -\nabla u$

The electric current density $J = \nabla \times \mathbf{H} = -\gamma \nabla u$

The governing equation is $\nabla \cdot (\gamma \nabla u) = 0$

The mathematical model

The continuum forward models for EIT

$$\nabla \cdot (\gamma \nabla u) = 0 \quad \text{in} \quad \Omega$$
$$u = V \quad \text{on} \quad \partial\Omega$$

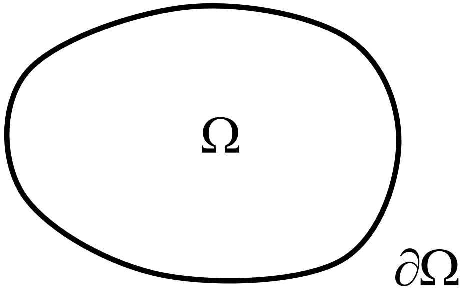

We may also have Neumann condition

$$\gamma \frac{\partial u}{\partial n} = I \quad \text{on} \quad \partial\Omega \quad \text{and} \quad \int_{\partial\Omega} I \; ds = 0$$

The DtN map $\Lambda_\gamma : H^{\frac{1}{2}}(\partial\Omega) \to H^{-\frac{1}{2}}(\partial\Omega)$ is defined as

$$\Lambda_\gamma V = \gamma \frac{\partial u}{\partial n}$$

Calderon: Given the DtN map Λ_γ, find γ.

Given partial, noisy knowledge of Λ_γ^{-1}, find γ.

Modeling the electrodes

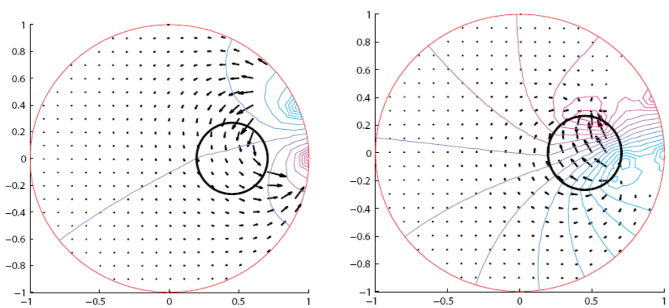

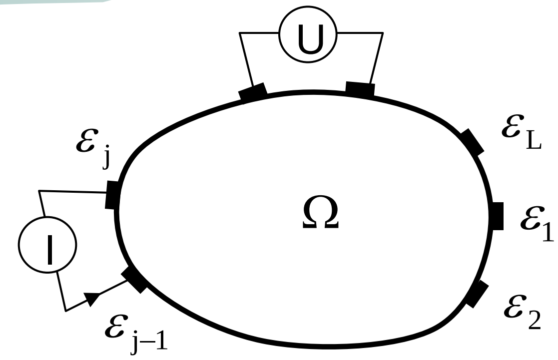

Using the complete electrode model the resulting time-harmonic voltage, denoted by $u^{j,\omega}$, satisfies

$$\begin{cases} \nabla \cdot (\gamma_\omega \nabla u^{j,\omega}) = 0 & \text{in } \Omega \\ (u^{j,\omega} + z_k \gamma_\omega \frac{\partial u^{j,\omega}}{\partial \mathbf{n}})|_{\mathcal{E}_k} = U_k^{j,\omega}, & k = 1, \cdots, L \\ \gamma_\omega \frac{\partial u^{j,\omega}}{\partial \mathbf{n}} = 0 & \text{on } \partial\Omega \setminus \cup_{k=1}^{L} \mathcal{E}_k \\ \int_{\mathcal{E}_k} \gamma_\omega \frac{\partial u^{j,\omega}}{\partial \mathbf{n}} = 0 & \text{if } \quad k \in \{1, \cdots, L\} \setminus \{j-1, \ j\} \\ \int_{\mathcal{E}_j} \gamma_\omega \frac{\partial u^{j,\omega}}{\partial \mathbf{n}} \ ds = I = -\int_{\mathcal{E}_{j-1}} \gamma_\omega \frac{\partial u^{j,\omega}}{\partial \mathbf{n}} \ ds \end{cases}$$

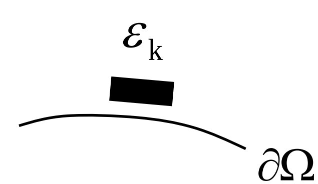

Inverse Problem

The inverse problem of EIT is to reconstruct images of conductivity σ and permittivity distributions ε inside the subject from current and voltage measurements of its boundary.

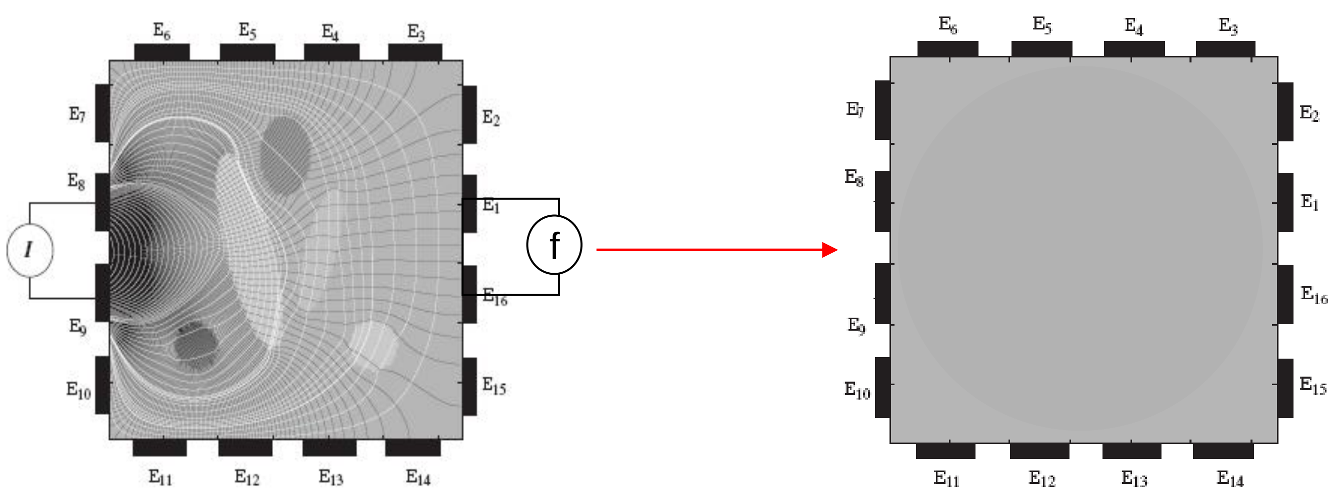

Static EIT reconstruction algorithm

Let $f^j := (U_1^j - U_L^j, \;\cdots,\; U_L^j - U_{L-1}^j) \in \mathbb{C}^L$, and
$u^{j,\gamma} := (u_1^j(\gamma) - u_L^j(\gamma), \;\cdots,\; u_L^j(\gamma) - u_{L-1}^j(\gamma)) \in \mathbb{C}^L$

$$\mathbf{f} = \underbrace{\left(f^1,\; f^2, \cdots, f^L\right)}_{\text{measured voltage set}}$$

$$\mathbf{u}(\gamma) = \underbrace{\left(u^{1,\gamma},\; u^{2,\gamma}, \cdots, u^{L,\gamma}\right)}_{\text{computed voltage set with } \gamma}$$

We try to find γ which minimizes the difference between computed data with γ and measured data:

$$\Phi(\gamma) = \|\mathbf{f} - \mathbf{u}(\gamma)\|^2 = \sum_{j=1}^{L} \sum_{k=1}^{L} \left| f_k^j - u_k^{j,\gamma} \right|^2$$

Numerical Algorithm

Gauss-Newton iteration:

Having the initial value $\gamma^{(0)}$ fixed, the Gauss-Newton step is

$$\gamma^{(i+1)} = \gamma^{(i)} - (\mathbf{H}^{(i)})^{-1} \nabla \Phi^{(i)}$$

where the Hessian $\mathbf{H}^{(i)} = (D\mathbf{u}(\gamma^{(i)}))^T D\mathbf{u}(\gamma^{(i)})$

and the gradient $\nabla \Phi^{(i)} = (D\mathbf{u}(\gamma^{(i)}))^T (\mathbf{u}(\gamma^{(i)}) - \mathbf{f})$

Gauss-Newton iteration for the least squares methods leads to

$$\int_\Omega \delta\gamma \nabla u^j \cdot \nabla u^k dx = I(f^j_{t_2} - f^j_{t_1}) \quad j, k = 1, 2, \cdots, L$$

4 Channel Example - Data Set

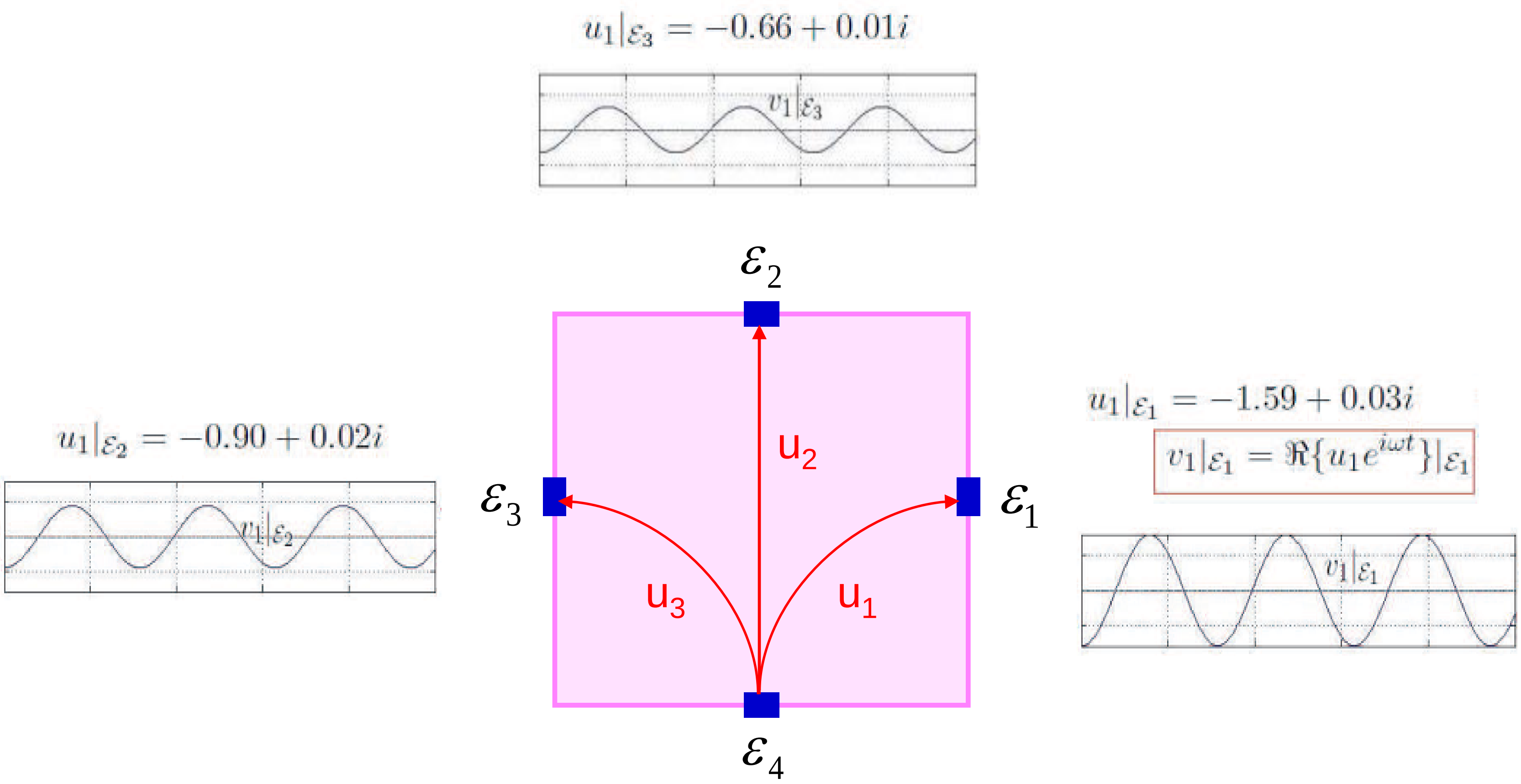

4 Channel Example – Inverse Problem

Reconstruction of γ in 4-channel EIT system:

Find a rough structure of γ from the following data set F.

	k=1	k=2	k=3
f_{1k}	-2.0285	-1.3025	-1.0962
f_{2k}	-1.3068	-2.3413	-1.3633
f_{3k}	-1.1053	-1.3724	-2.5987

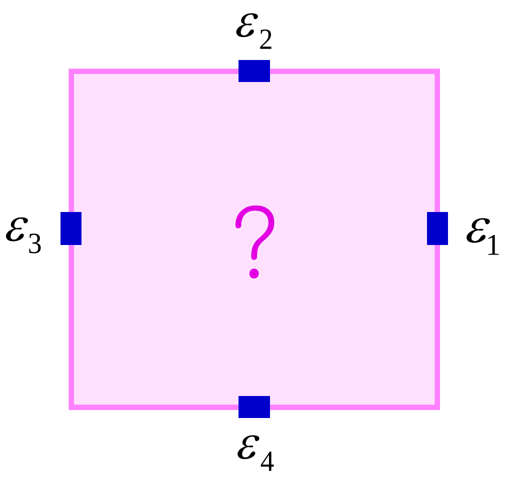

Simulate NtD data for a given conductivity

For the given injection current $I_j (j = 1, 2, 3)$,
we compute the complex potential u_j satisfying

$$\mathcal{P}_j[\gamma] : \begin{cases} \nabla \cdot (\gamma \nabla u_j) = 0 \text{ in } \Omega \\ \int_{\mathcal{E}_4} \gamma \frac{\partial u_j}{\partial n} = I = -\int_{\mathcal{E}_j} \gamma \frac{\partial u_j}{\partial n} \\ \gamma \frac{\partial u_j}{\partial n} = 0 \text{ on } \partial\Omega \setminus (\mathcal{E}_j \cup \mathcal{E}_4) \\ \nabla u_j \times n = 0 \text{ on } \mathcal{E}_j \text{ and } u_j = 0 \text{ on } \mathcal{E}_4 \end{cases}$$

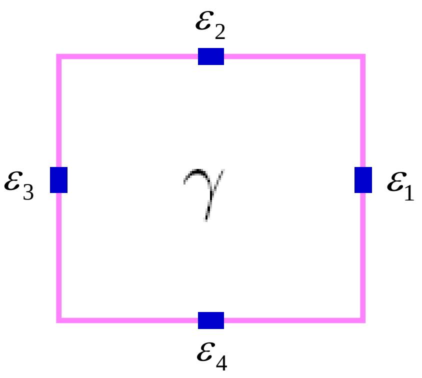

By solving $\mathcal{P}_j[\gamma]$, we obtain the simulated NtD data:

1st current:	$u_1(\gamma)\|_{\mathcal{E}_1}$	$u_1(\gamma)\|_{\mathcal{E}_2}$	$u_1(\gamma)\|_{\mathcal{E}_3}$
2nd current:	$u_2(\gamma)\|_{\mathcal{E}_1}$	$u_2(\gamma)\|_{\mathcal{E}_2}$	$u_2(\gamma)\|_{\mathcal{E}_3}$
3rd current:	$u_3(\gamma)\|_{\mathcal{E}_1}$	$u_3(\gamma)\|_{\mathcal{E}_2}$	$u_3(\gamma)\|_{\mathcal{E}_3}$

4 Channel Example – Forward Solver

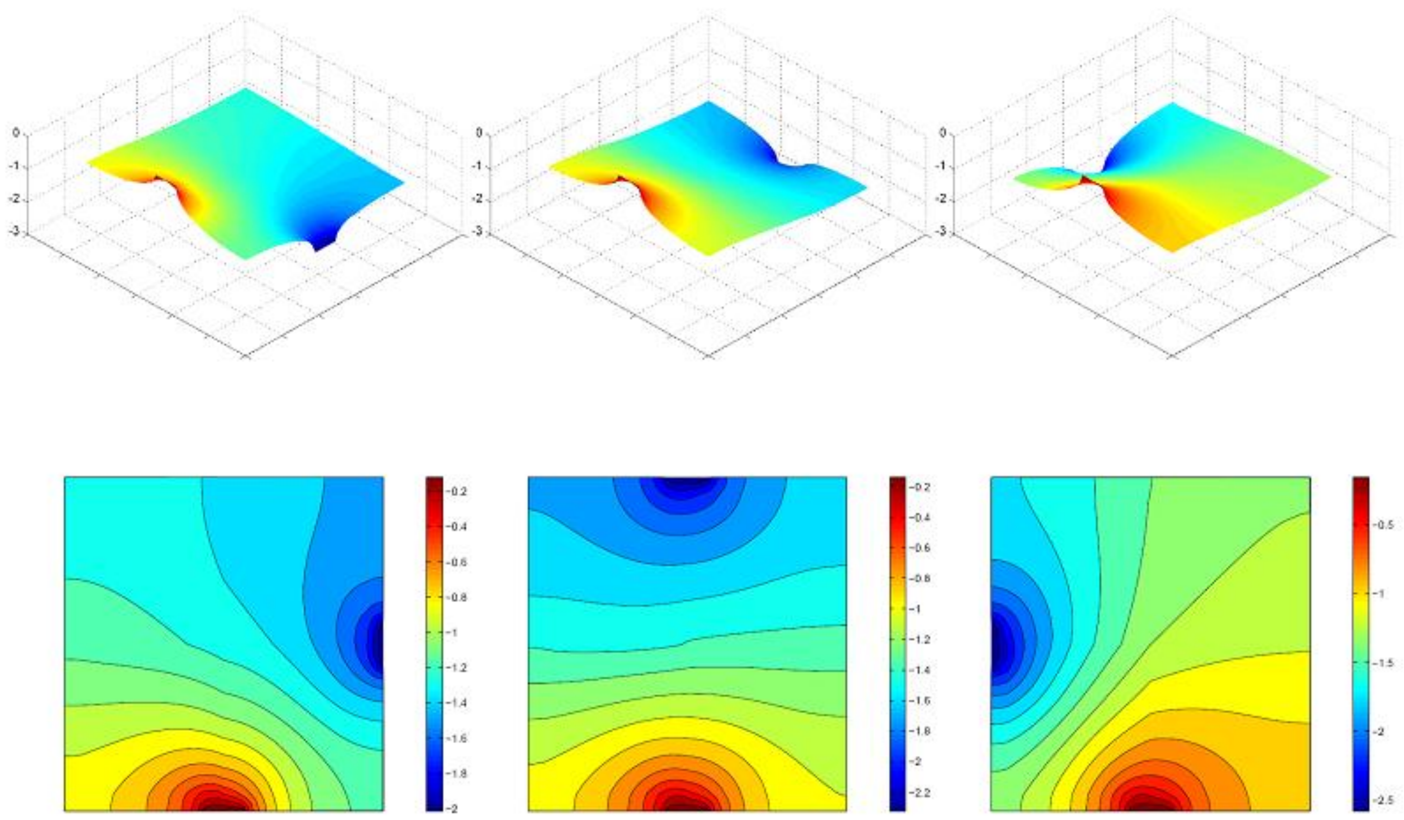

1st current   2nd current   3rd current

4 Channel Example - Reconstruction Method

Let $u_j(\gamma)$ be the solution of the direct problem $\mathcal{P}_j[\gamma]$.

$$\mathbf{f} := \underbrace{\begin{bmatrix} f_{11} & f_{12} & f_{13} \\ f_{21} & f_{21} & f_{23} \\ f_{32} & f_{32} & f_{33} \end{bmatrix}}_{\text{measured voltage set}} \qquad \mathbf{u}(\gamma) := \underbrace{\begin{bmatrix} u_1(\gamma)|_{\mathcal{E}_1} & u_1(\gamma)|_{\mathcal{E}_2} & u_1(\gamma)|_{\mathcal{E}_3} \\ u_2(\gamma)|_{\mathcal{E}_1} & u_2(\gamma)|_{\mathcal{E}_2} & u_2(\gamma)|_{\mathcal{E}_3} \\ u_3(\gamma)|_{\mathcal{E}_1} & u_3(\gamma)|_{\mathcal{E}_2} & u_3(\gamma)|_{\mathcal{E}_3} \end{bmatrix}}_{\text{computed voltage set with } \gamma}$$

We try to find γ which minimizes the difference between computed data with γ and measured data:

$$\Phi(\gamma) = \|\mathbf{f} - \mathbf{u}(\gamma)\|^2 = \sum_{j=1}^{3} \sum_{k=1}^{3} |f_{jk} - u_j(\gamma)|_{\mathcal{E}_k}|^2$$

Gauss-Newton iteration for the least squares problem yields:

$$\int_\Omega \delta\gamma \nabla u_j(\gamma) \cdot \nabla u_k(\gamma) dx = u_j(\gamma)|_{\mathcal{E}_k} - f_{jk} \quad j, k = 1, 2, 3$$

Reciprocity theorem

Reciprocity property: $f_{kj} = f_{j\,k}$

The reciprocity property yields that

$$\mathbf{f} := \begin{bmatrix} f_{11} & f_{12} & f_{13} \\ f_{21} & f_{21} & f_{23} \\ f_{32} & f_{32} & f_{33} \end{bmatrix}$$

is symmetric

In $(L+1)$ channel EIT system, we collect L^2 data,

and the number of independent data is $L(L+1)/2$.

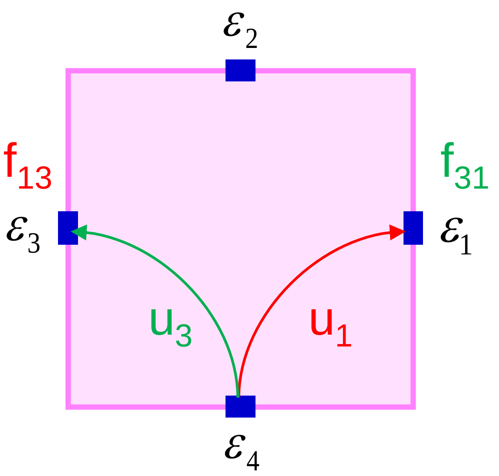

4 Channel Example - Algorithm

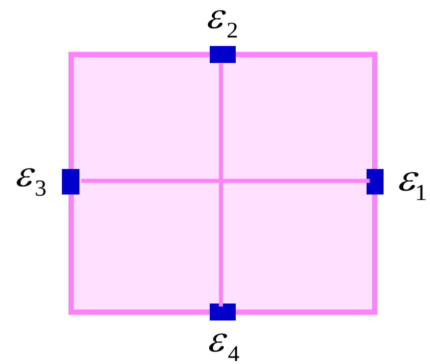

Divide Ω into $\Omega = \Omega_1 \cup \Omega_2 \cup \cdots \cup \Omega_N$.

Assume that γ is a constant on each Ω_m, $m = 1, 2, \cdots, N$.

Write it as a matrix form $\mathcal{A}\mathbf{x} = \mathbf{b}$.

$$\begin{pmatrix} \int_{\Omega_1} \nabla u_1 \cdot \nabla u_1 \cdots \int_{\Omega_N} \nabla u_1 \cdot \nabla u_1 \\ \int_{\Omega_1} \nabla u_1 \cdot \nabla u_2 \cdots \int_{\Omega_N} \nabla u_1 \cdot \nabla u_2 \\ \int_{\Omega_1} \nabla u_1 \cdot \nabla u_3 \cdots \int_{\Omega_N} \nabla u_1 \cdot \nabla u_3 \\ \int_{\Omega_1} \nabla u_2 \cdot \nabla u_1 \cdots \int_{\Omega_N} \nabla u_2 \cdot \nabla u_1 \\ \int_{\Omega_1} \nabla u_2 \cdot \nabla u_2 \cdots \int_{\Omega_N} \nabla u_2 \cdot \nabla u_2 \\ \int_{\Omega_1} \nabla u_3 \cdot \nabla u_1 \cdots \int_{\Omega_N} \nabla u_3 \cdot \nabla u_1 \end{pmatrix} \begin{pmatrix} \delta\gamma_1 \\ \delta\gamma_2 \\ \vdots \\ \vdots \\ \delta\gamma_N \end{pmatrix} = \begin{pmatrix} u_1(\gamma)|_{\mathcal{E}_1} - f_{11} \\ u_1(\gamma)|_{\mathcal{E}_2} - f_{12} \\ u_1(\gamma)|_{\mathcal{E}_3} - f_{13} \\ u_2(\gamma)|_{\mathcal{E}_2} - f_{22} \\ u_2(\gamma)|_{\mathcal{E}_3} - f_{23} \\ u_3(\gamma)|_{\mathcal{E}_3} - f_{33} \end{pmatrix}$$

4 Channel Example - Simulation

Algorithm

1. Start with the initial guess $\gamma = 1$.
2. Solve the forward problem $\mathcal{P}[\gamma]$.
3. Compute $\delta\gamma$ using $\int_\Omega \delta\gamma \nabla u_j(\gamma) \cdot \nabla u_k(\gamma) dx = u_j(\gamma)|_{\mathcal{E}_k} - f_{jk}$.
4. Update $\gamma + \delta\gamma$.
5. Repeat the process 2,3, and 4 with updated γ

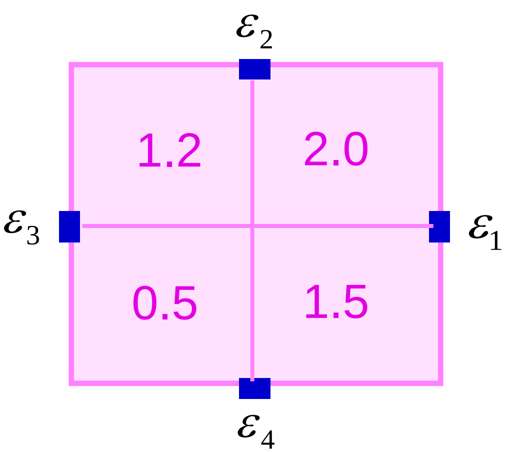

Iteration	Ω_1	Ω_2	Ω_3	Ω_4
0	1	1	1	1
1	0.6023	1.2830	1.1144	1.5003
2	0.5321	1.4344	1.1680	1.8279
3	0.5083	1.4852	1.1917	1.9558
4	0.5020	1.4971	1.1981	1.9901
5	0.5005	1.4994	1.1996	1.9979
True	0.5	1.5	1.2	2.0

4 Channel Example - Simulation

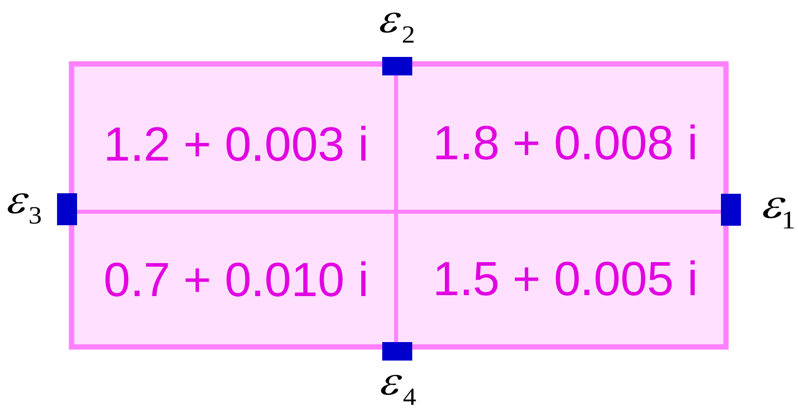

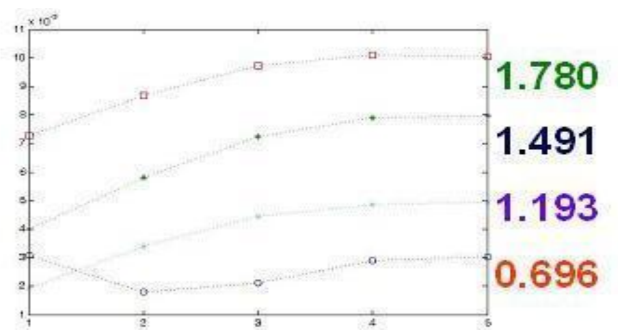

real part after 5 iterations

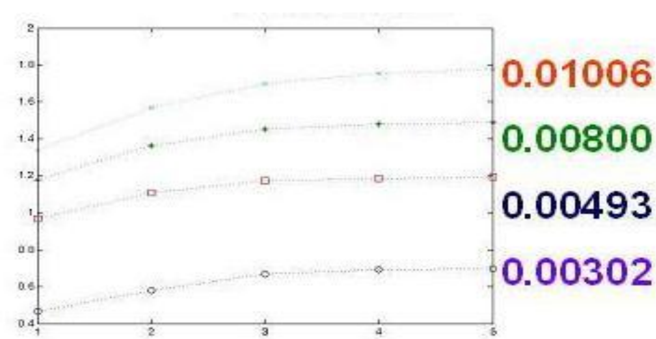

imaginary part after 5 iterations

Effect of a geometry error in static EIT

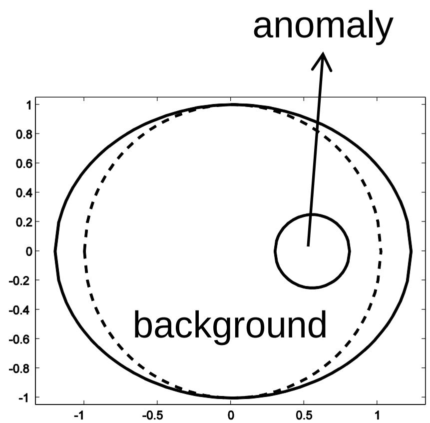

(a) object

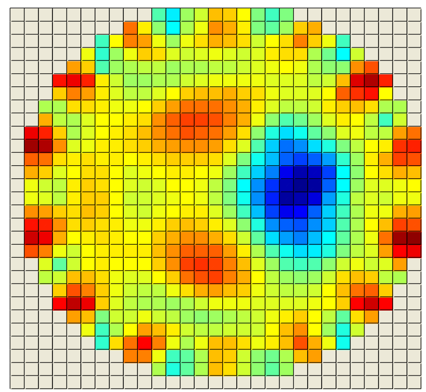

(b) 100 Hz

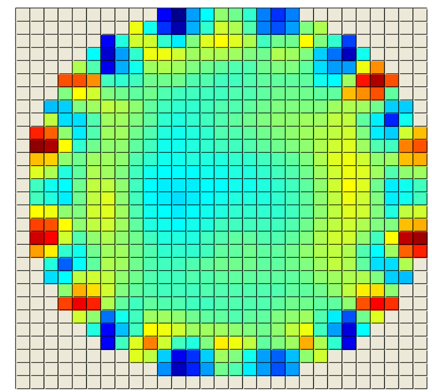

(c) 50 kHz

Effect of a boundary geometry error in static EIT:

The ellipse is the true domain and the circle is the computational domain in (a).

(b),(c) are reconstructed static images at frequencies of 100 Hz and 50 kHz.

Time difference EIT (tdEIT)

Reconstruction Algorithm

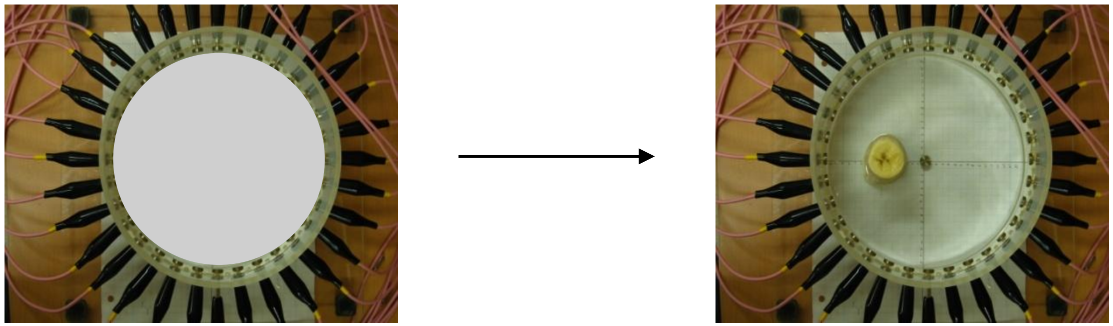

In FdEIT, we try to reconstruct time-difference images of $\delta\gamma$ minimizing the following functional:

$$\Phi(\delta\gamma) = \| \, \delta\mathbf{u} - (\mathbf{f}_{t_2} - \mathbf{f}_{t_1}) \, \|^2$$

Gauss-Newton iteration for the least squares method leads to

$$\int_{\Omega} \delta\gamma \nabla u^j \cdot \nabla u^k \, dx = \int_{\partial\Omega} (f^j_{t_1} - f^j_{t_2}) g^k \, ds$$

Phantom experiments - tdEIT

conductivity

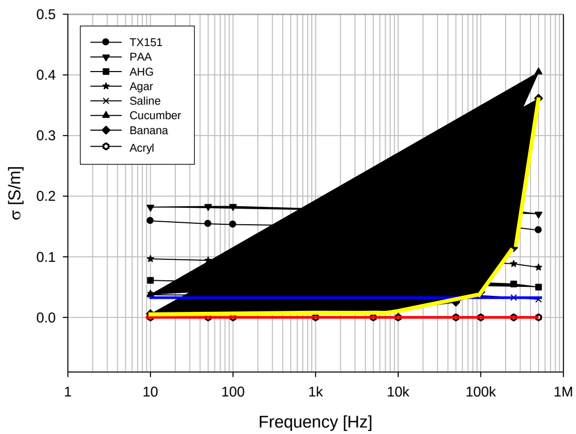

permittivity

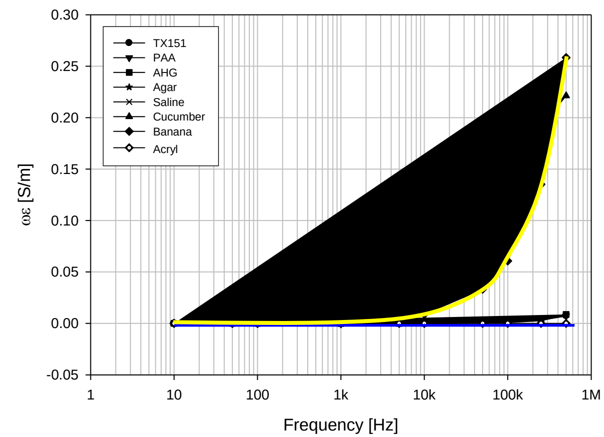

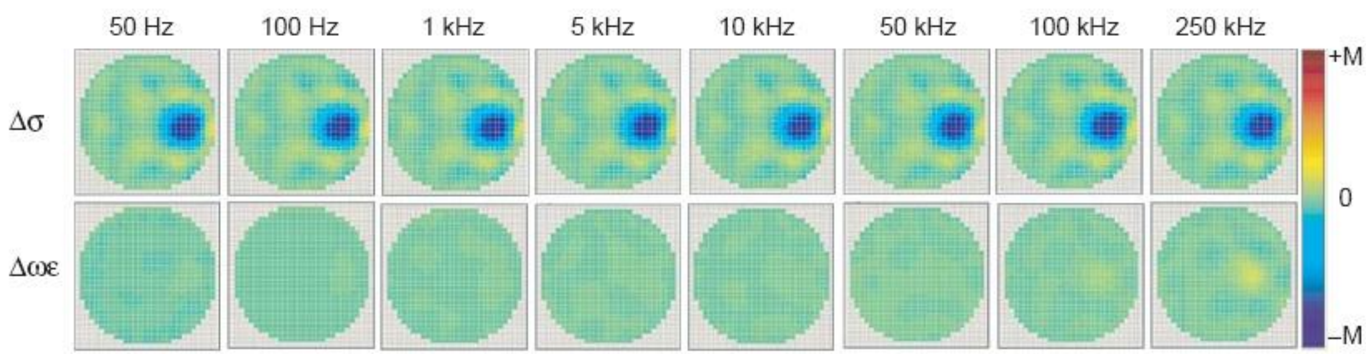

Imaging experiments using a phantom including an anomaly of acryl in a saline background.

Phantom experiments - tdEIT

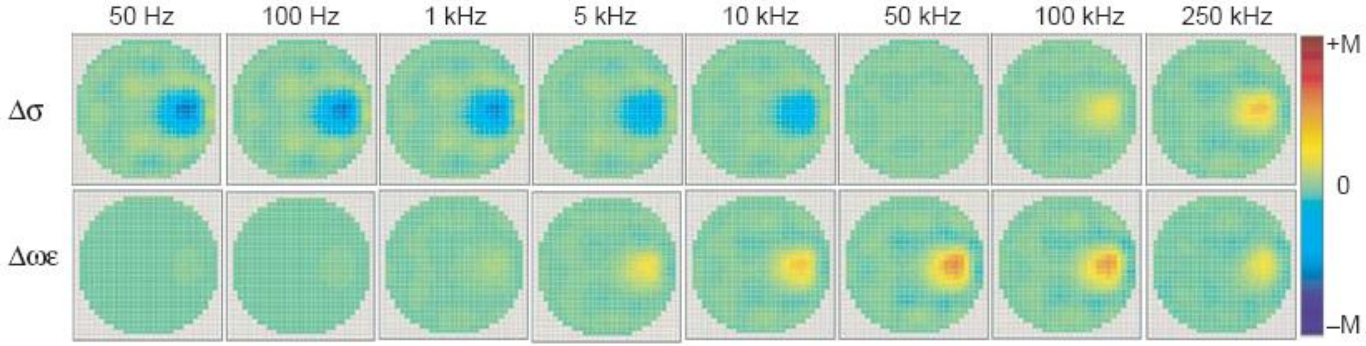

Imaging experiments using a phantom including an anomaly of banana in a saline background.

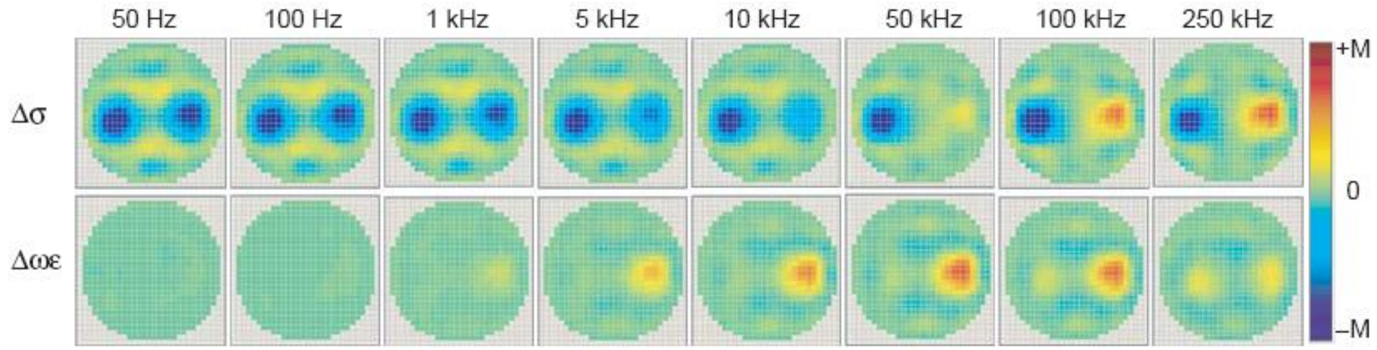

Imaging experiments using a phantom including an anomaly of acryl and banana in a saline background.

Applications - tdEIT

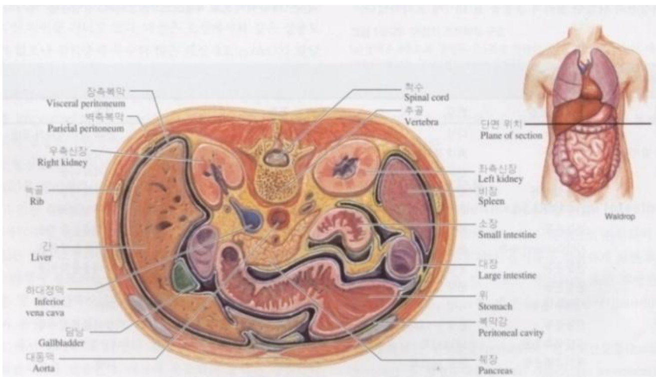

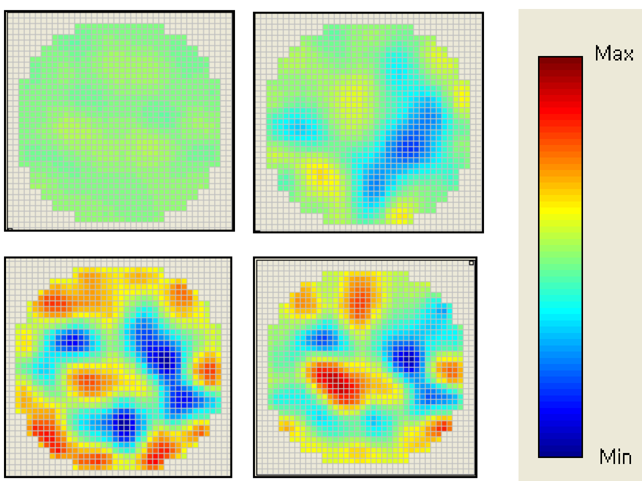

Imaging gastric emptying

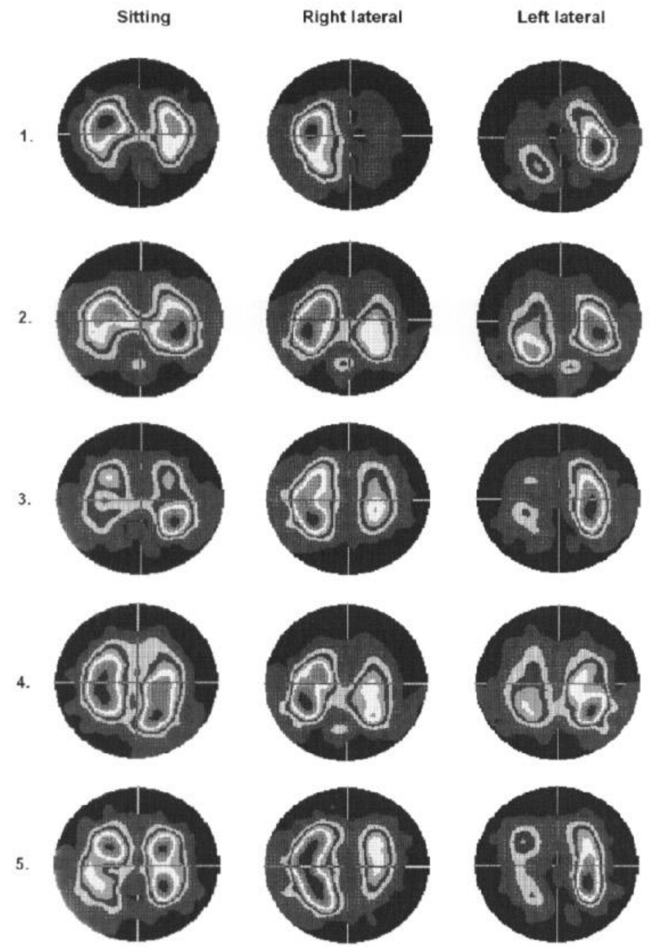

Monitoring of pulmonary function

Applications where reference is not available


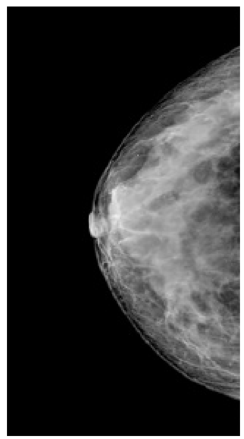

Mammography

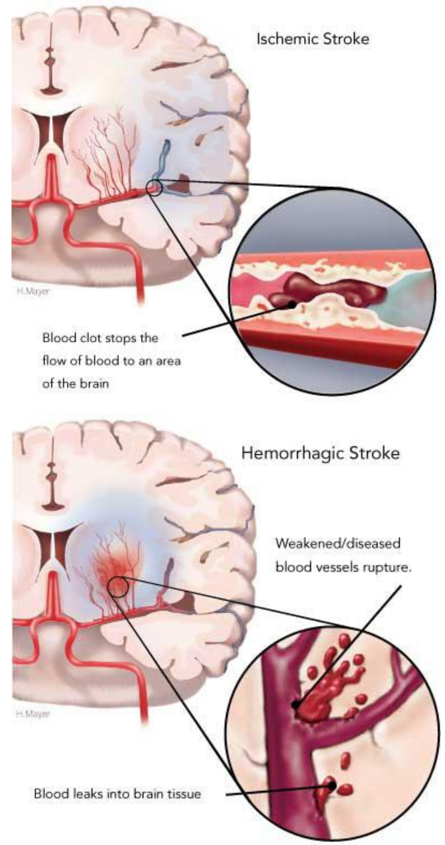

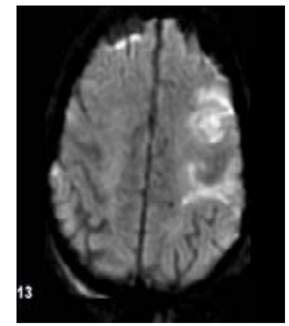

ischemic stroke

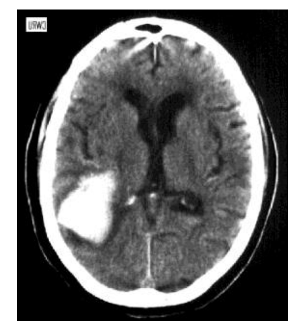

hemorrhagic stroke

In EIT for breast cancer detection or urgent neuroimaging in acute stroke, background NtD data is not available.

Frequency difference EIT (FdEIT)

Complex conductivity spectra

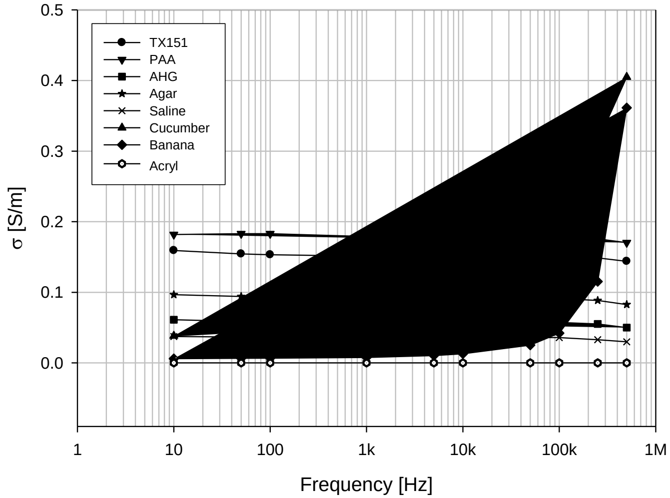

conductivity

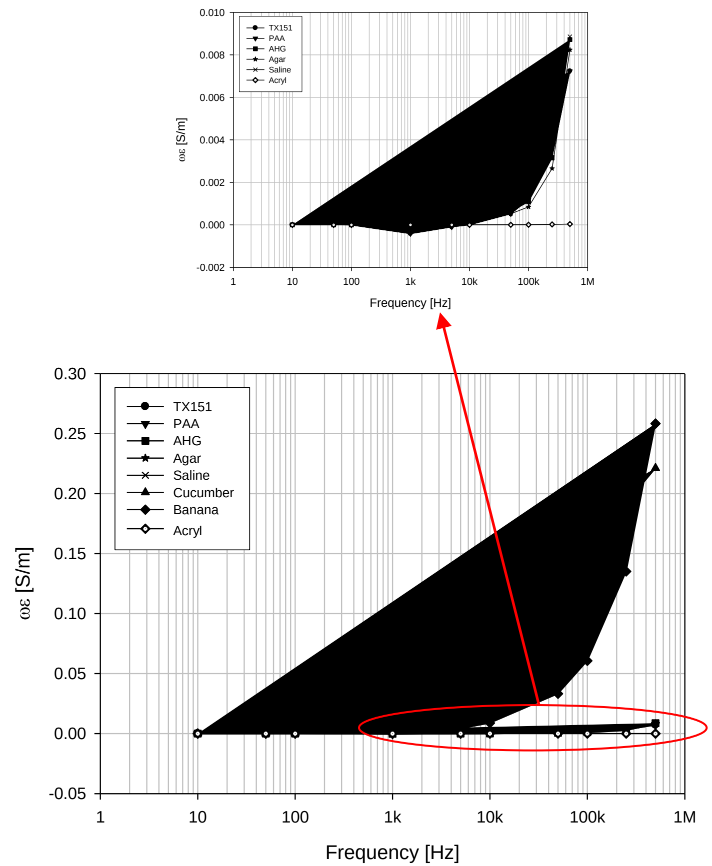

permittivity

FdEIT using simple difference

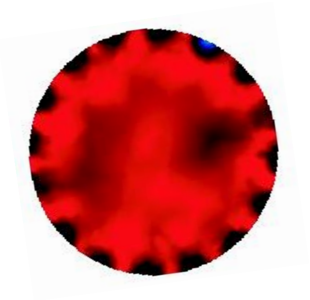

Phantom including an anomaly of banana in a saline background:

While the anomaly is frequency dependent, the saline background is almost frequency independent. And the simple difference works well.

Phantom including an anomaly of potato in a carrot background:

Since the carrot background is frequency dependent, the voltage difference is dominated by background conductivity including boundary geometry.

Why weighted difference is essential?

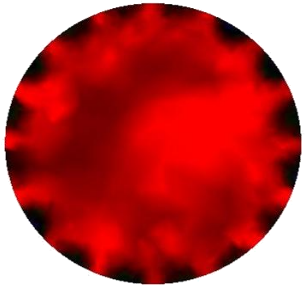

In the homogeneous object, the two vectors $\mathbf{f}_{\omega_1}$ and $\mathbf{f}_{\omega_2}$ are parallel in such a way that

$$\mathbf{f}_{\omega_2} = \frac{\gamma_{\omega_1}}{\gamma_{\omega_2}} \mathbf{f}_{\omega_1}$$

When there exists a small anomaly inside the imaging object, the difference $\mathbf{f}_{\omega_2} - \mathbf{f}_{\omega_1}$ significantly depends on the boundary geometry and electrode positions except the special case where $\mathbf{f}_{\omega_2} - \mathbf{f}_{\omega_1} = 0$.

Key idea of the weighted difference

We assume that there exist two appropriate frequencies ω_1 and ω_2 and a complex number α_b satisfying the following two conditions:

1. In the region near the boundary, especially near the sensing electrodes, the weighted difference of the complex conductivities at ω_1 and ω_2 is negligibly small, that is,

   $$\delta\gamma_{\omega_1}^{\omega_2}(\mathbf{r}) = \alpha_b \gamma_{\omega_2} - \gamma_{\omega_1} \approx 0 \quad \longrightarrow \quad \alpha_b \approx \frac{\gamma_{\omega_1}}{\gamma_{\omega_2}}$$

   Here γ_{ω_1} and γ_{ω_2} are the complex conductivities of background at frequency ω_1 and ω_2, respectively.

2. The magnitude $|\delta\gamma_{\omega_1}^{\omega_2}(\mathbf{r})|$ in the anomaly is bigger than that in the background region.

Sensitivity analysis

The following representation formula explains how the weighted frequency-difference data $f_{\omega_2} - \alpha_b f_{\omega_1}$ is related to the anomaly.

$$f_{\omega_2}(\mathbf{r}) - \alpha_b f_{\omega_1}(\mathbf{r}) = \int_D \frac{\mathbf{r}-\mathbf{r}'}{\pi|\mathbf{r}-\mathbf{r}'|^2} \cdot \left[\tau_2 \nabla u_{\omega_2}(\mathbf{r}') - \tau_1 \nabla u_{\omega_1}(\mathbf{r}')\right] d\mathbf{r}'$$

where

$$\alpha_b = \frac{\sigma_b(\omega_1) + i\omega_1 \epsilon_b(\omega_1)}{\sigma_b(\omega_2) + i\omega_2 \epsilon_b(\omega_2)}$$

and

$$\tau_j = \frac{(\sigma_b(\omega_j) - \sigma_a(\omega_j)) + i\omega_j(\epsilon_b(\omega_j) - \epsilon_a(\omega_j))}{\sigma_b(\omega_2) + i\omega_2 \epsilon_b(\omega_2)}, \; j = 1, 2.$$

Mechanisms of image contrast

- contrast in complex conductivity between an anomaly and background
- frequency-dependency of a complex conductivity distribution

We can detect D even for the case where $\sigma_l(\omega_1) = \sigma_l(\omega_2)$ and $\epsilon_l(\omega_1) = \epsilon_l(\omega_2)$ for $l = a, b$ (no changes in conductivity and permittivity with respect to frequency). In this case, the imaginary part of the formula can be simplified as

$$\Im\{f_{\omega_2}(\mathbf{r}_j) - \alpha_b f_{\omega_1}(\mathbf{r}_j)\} \approx |D| \left[\frac{\omega_2 \epsilon_b}{\sigma_b} \left(\frac{\sigma_a}{\sigma_b} - \frac{\epsilon_a}{\epsilon_b} \right) \frac{(\mathbf{z}-\mathbf{r}_j)\cdot\nabla v_1(\mathbf{z})}{|\mathbf{z}-\mathbf{r}_j|^2} \right]$$

where $\mathbf{r}_j$ is the center of the electrode $\mathcal{E}_j$ for each $j = 1, \cdots, L$ and $\mathbf{z}$ the center of D. Hence, we can still detect D provided that $\frac{\sigma_a}{\sigma_b} \neq \frac{\epsilon_a}{\epsilon_b}$.

Numerical simulation

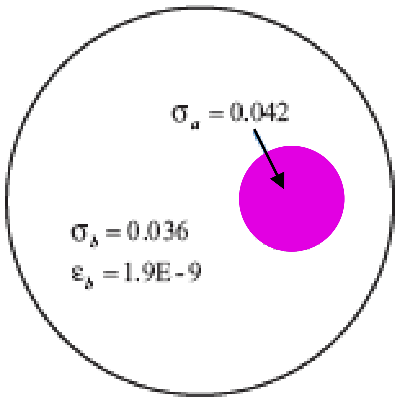

reconstructed fdEIT images in case of

$\sigma(\omega_1) = \sigma(\omega_2)$ and $\epsilon(\omega_1) = \epsilon(\omega_2)$

for $\omega_1/2\pi = 1$ kHz and $\omega_2/2\pi = 100$ kHz.

$\varepsilon_a = 9.7E-9$		$\varepsilon_a = 2.2E-9$
$\Re\{\alpha_b \gamma_{\omega_2} - \gamma_{\omega_1}\}$	$\Im\{\alpha_b \gamma_{\omega_2} - \gamma_{\omega_1}\}$	$\lvert\alpha_b \gamma_{\omega_2} - \gamma_{\omega_1}\rvert$
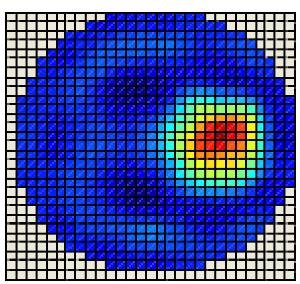	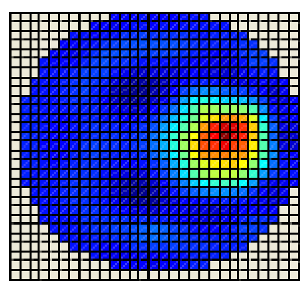	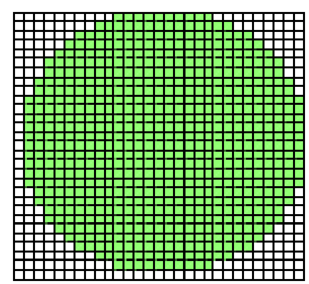

FdEIT reconstruction algorithm

The reconstruction uses the least square method for the misfit functional

$$\Psi(\delta\gamma) = \sum_{j=1}^{L} \int_{\partial\Omega} \left| \delta U^j - (f^j_{\omega_2} - \alpha_b f^j_{\omega_1}) \right|^2 ds$$

Using the fact that $\nabla \cdot \left(\delta\gamma \nabla u^j_{\omega_1} \right) = \nabla \cdot (\alpha_b^{-1} (\gamma_{\omega_1} + \delta\gamma) \nabla \delta u^j)$,

$$\int_\Omega (\alpha_b \gamma_{\omega_2} - \gamma_{\omega_1}) \nabla u^j_{\omega_1} \cdot \nabla u^k_{\omega_2} \, d\mathbf{r} = I \left(f^j_{\omega_2} - \alpha_b f^j_{\omega_1} \right)$$

We replace the term $u^j_{\omega_1}$ and $u^k_{\omega_2}$ by $\hat{u}^j_1$ and $\hat{u}^k_2$ and since $\hat{\gamma}_l \hat{u}^k_l = \hat{u}^j_0$ where $\hat{u}^j_0$ be a solution with $\gamma_\omega = 1$,

$$\int_\Omega (\alpha_b \gamma_{\omega_2} - \gamma_{\omega_1}) \nabla \left(\frac{\hat{u}^j_0}{\hat{\gamma}_1} \right) \cdot \nabla \left(\frac{\hat{u}^k_0}{\hat{\gamma}_2} \right) \, d\mathbf{r} \approx I \left(f^j_{\omega_2} - \alpha_b f^j_{\omega_1} \right)$$

Weights in fdEIT

As the complex conductivity is changed linearly from γ to $\alpha\gamma$, the corresponding voltage changes from f_ω to $\frac{1}{\alpha} f_\omega$. To get rid of the background component from f_{ω_2}, we decompose f_{ω_2} as:

$$f_{\omega_2} = \alpha_b f_{\omega_1} + h_{\omega_2}, \qquad \alpha_b = \frac{\langle f_{\omega_2}, f_{\omega_1} \rangle}{\langle f_{\omega_1}, f_{\omega_1} \rangle}$$

To compute the equivalent constant conductivity $\hat{\gamma}_\omega$ corresponding to γ_ω, we use the following relation:

$$\frac{\hat{\gamma}_\omega}{\hat{\gamma}_0} = \frac{\hat{\gamma}_\omega \int_\Omega \nabla u^{k,\omega} \cdot \nabla u^{j,0}}{\hat{\gamma}_0 \int_\Omega \nabla u^{k,\omega} \cdot \nabla u^{j,0}}$$

Applying the divergence theorem

$$\frac{\hat{\gamma}_\omega}{\hat{\gamma}_0} = \textit{average of } \frac{f_k^{j,0}}{f_j^{k,\omega}}$$

Robustness of fdEIT

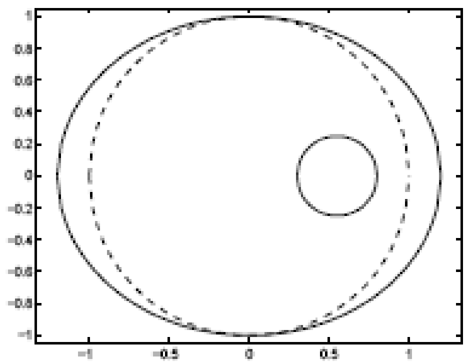

(a) object

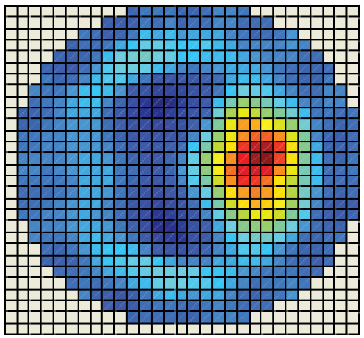

(b) fdEIT image

Effect of a boundary geometry error:
The ellipse is the true domain and the dotted circle is the computational domain in (a). (b) and (c) are reconstructed fdEIT and static EIT images, respectively at frequencies of 100 Hz and 50 kHz.

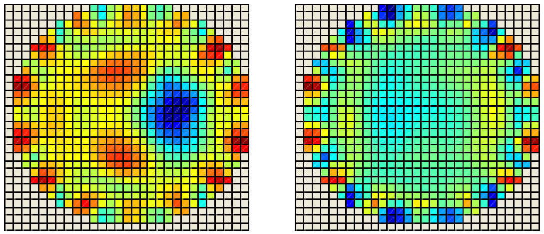

(c) static EIT images

Numerical simulation - 2D

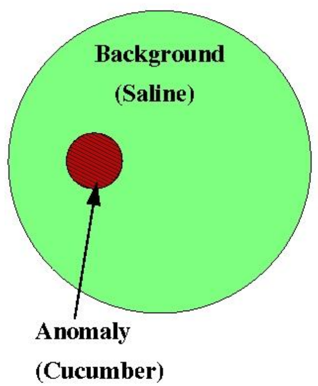

Frequency	Conductivity (10^{-2} S/m)	
	Saline	Cucumber
1 kHz	3.6	4.4 + 0.413 i
5 kHz	3.6 + 0.0024 i	5.1 + 1.51 i
50 kHz	3.6 + 0.0594 i	10.5 + 7.59 i

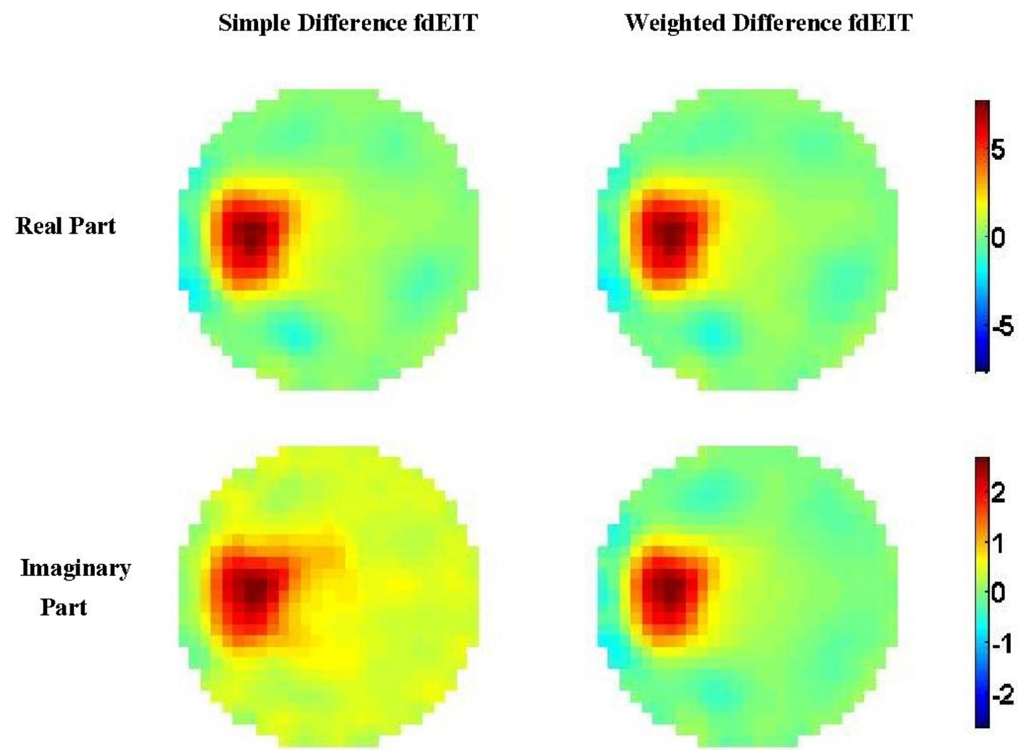

Numerical simulations of fdEIT image reconstructions using an imaging object including an anomaly of cucumber in a saline background. The simple difference produced similar fdEIT images to those by using the weighted difference since the background complex conductivity did not change much with frequency.

Numerical simulation - 2D

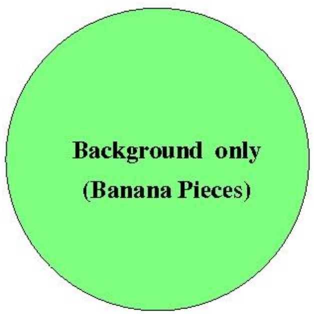

Frequency	Conductivity (10^{-2} S/m) Banana(pieces)
1 kHz	22.09 +10.90 i
5 kHz	22.78 + 9.68 i
50 kHz	28.29 + 15.00 i

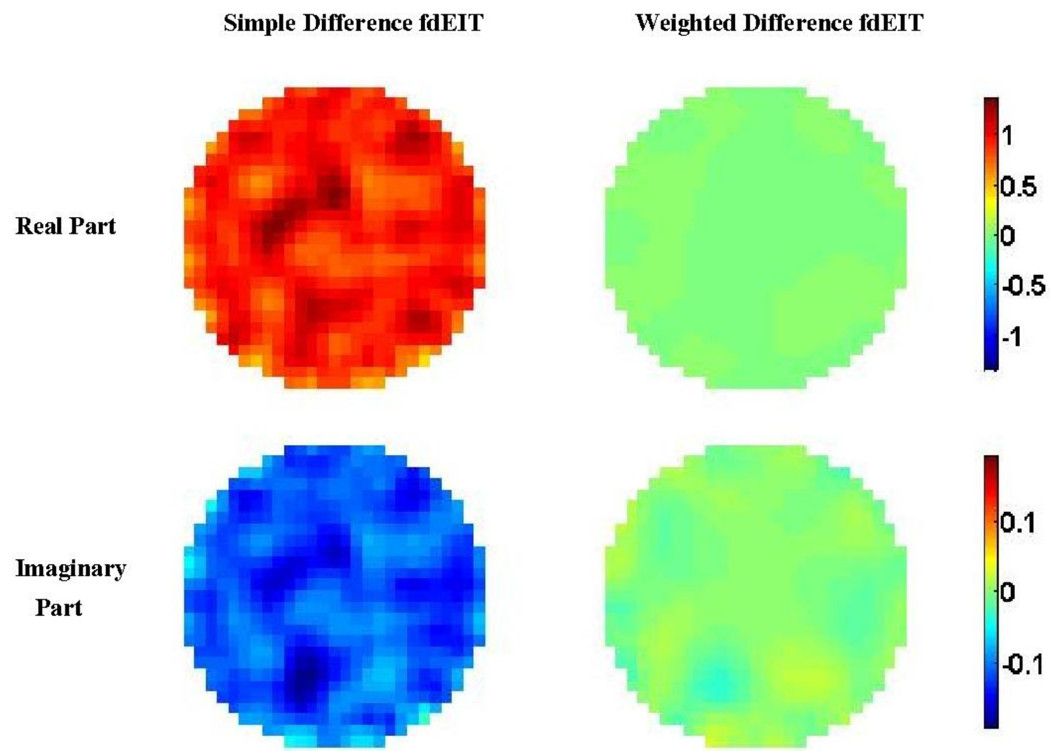

Numerical simulations of fdEIT image reconstructions using a homogeneous imaging object whose complex conductivity value changes with frequency. Reconstructed fdEIT images using the simple difference show severe artifacts even for a homogeneous case while images using the weighted difference are free from artifacts.

Numerical simulation - 2D

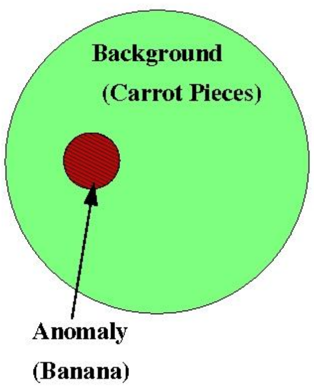

Frequency	Conductivity (10^{-2} S/m)	
	Carrot(pieces)	Banana
1 kHz	20.77 + 10.20 i	3.45 + 1.60 i
5 kHz	20.73 + 8.81 i	4.31 + 1.73 i
50 kHz	23.17 + 12.30 i	10.22 + 5.15 i

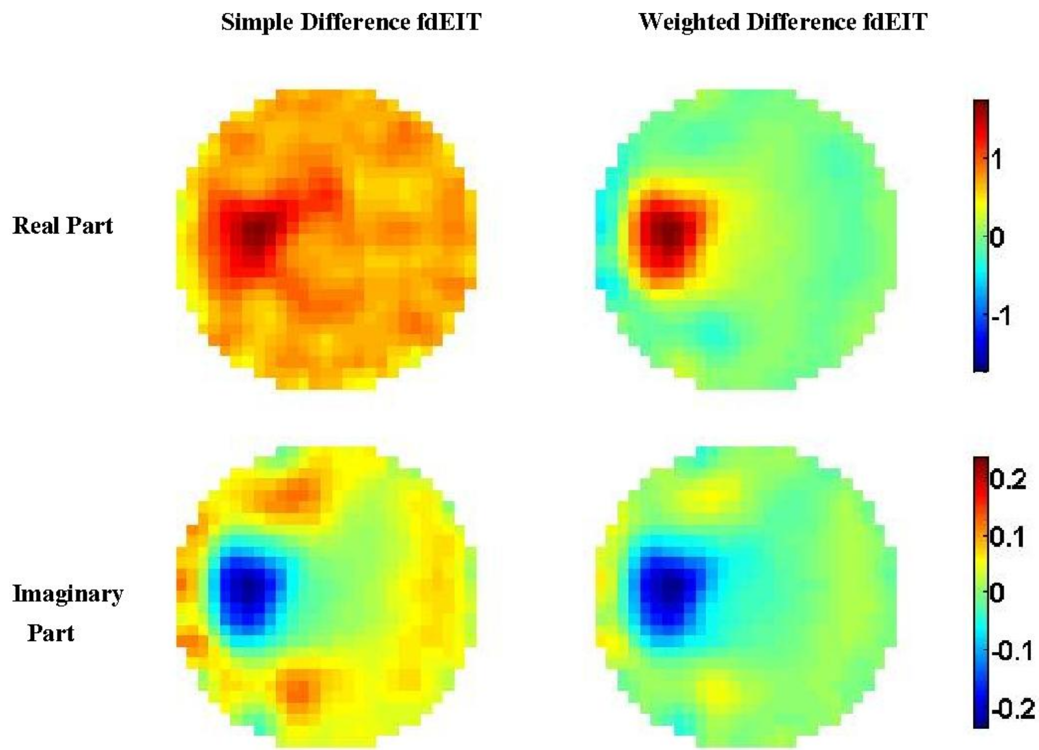

Numerical simulations of fdEIT image reconstructions using an imaging object including an anomaly of banana in a background of carrot pieces. The weighted difference produces meaningful fdEIT images while the simple difference failed to extract the contrast between the anomaly and the background .

Phantom experiments

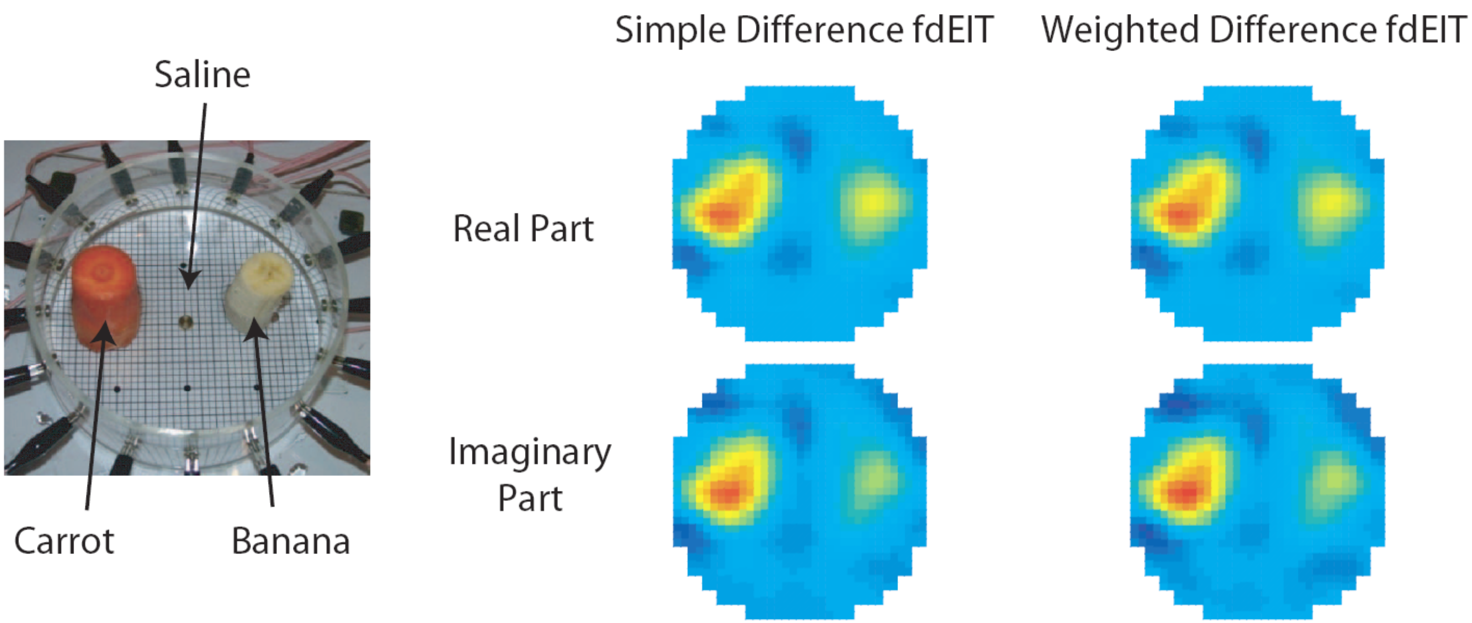

Imaging experiments using a phantom including two anomalies of carrot and banana in a saline background. Both of simple and weighted difference successfully produces fdEIT images since the background complex conductivity did not change much with frequency.

Phantom experiments

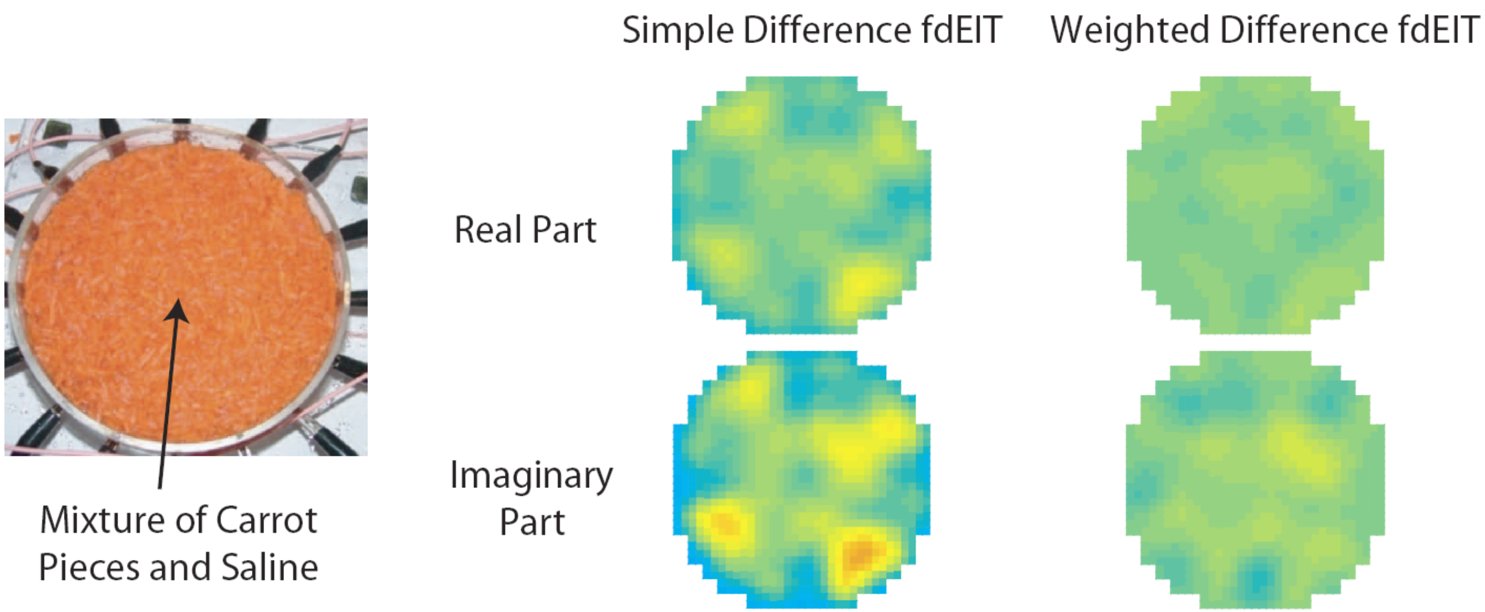

Imaging experiments using a homogeneous phantom filled with carrot pieces. Its complex conductivity changes with frequency and the simple difference produced fdEIT images with bigger artifacts compared with those using the weighted difference.

Phantom experiments

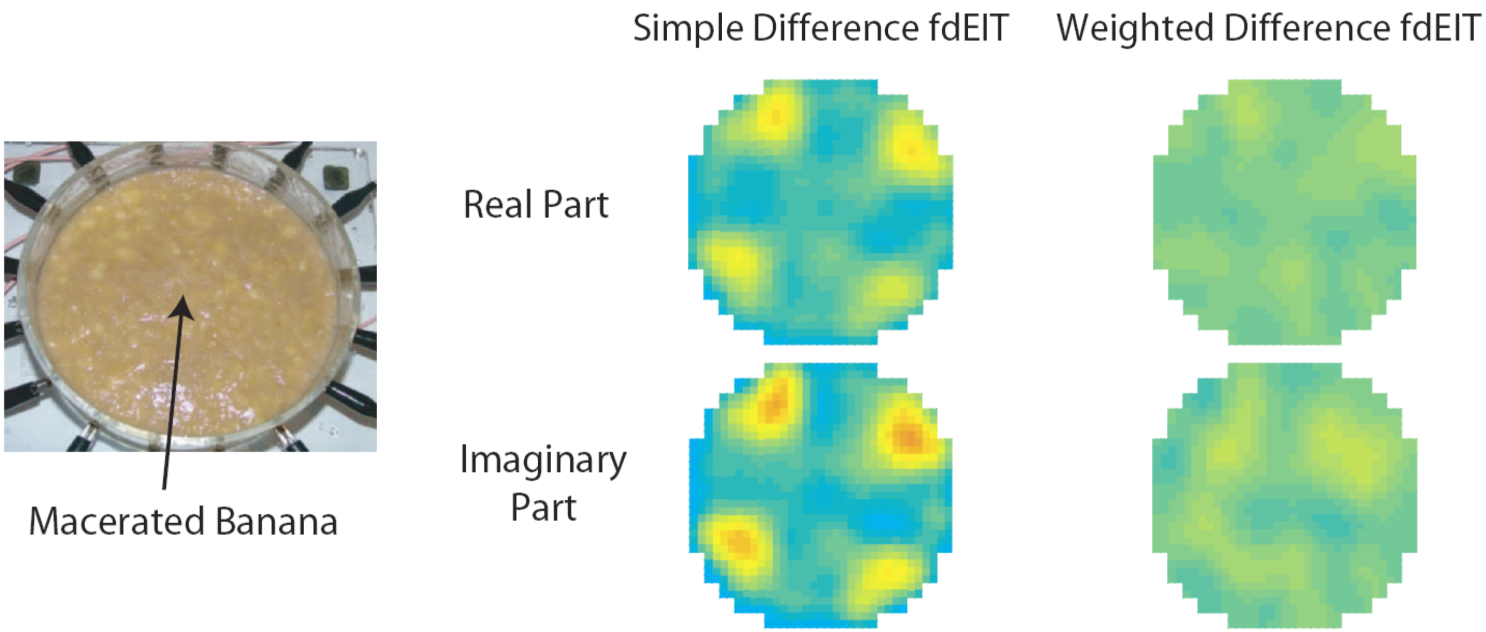

Imaging experiments using a homogeneous phantom filled with macerated banana. Its complex conductivity changes with frequency and the simple difference produced fdEIT images with bigger artifacts compared with those using the weighted difference.

Phantom experiments

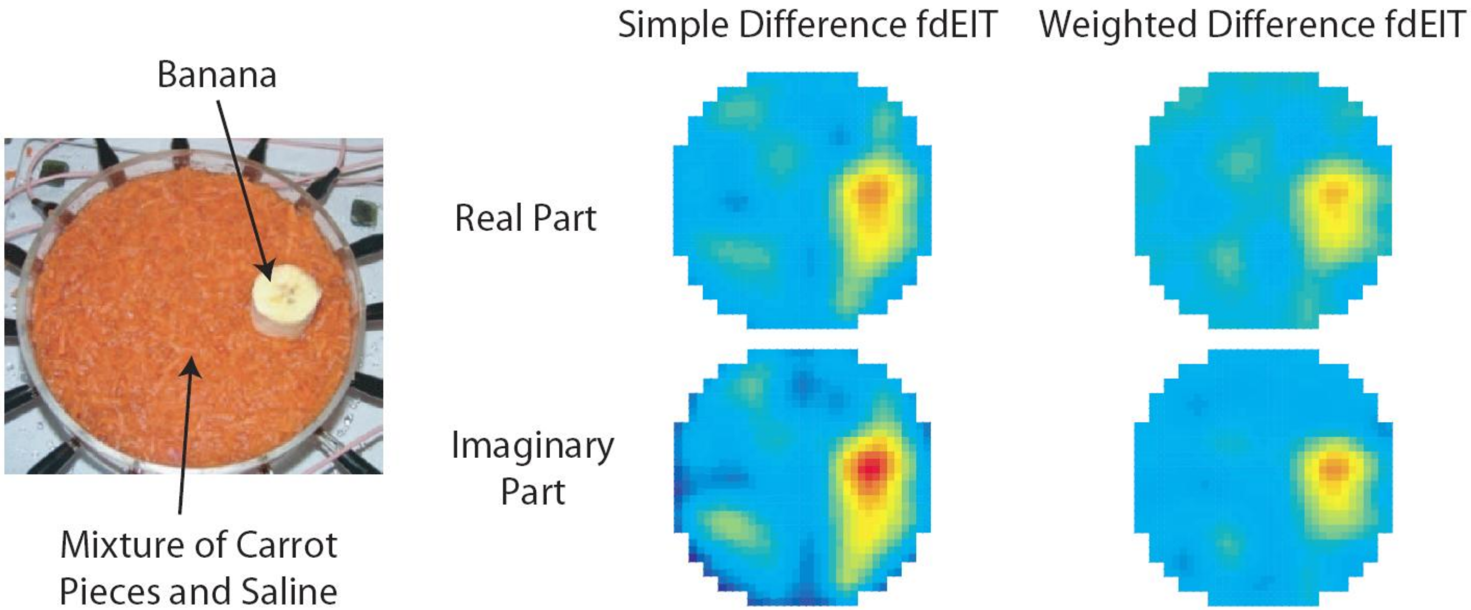

Imaging experiments using a homogeneous phantom including an anomaly of banana in a background of carrot pieces. The amounts artifacts are bigger in images using the simple difference.

Phantom experiments

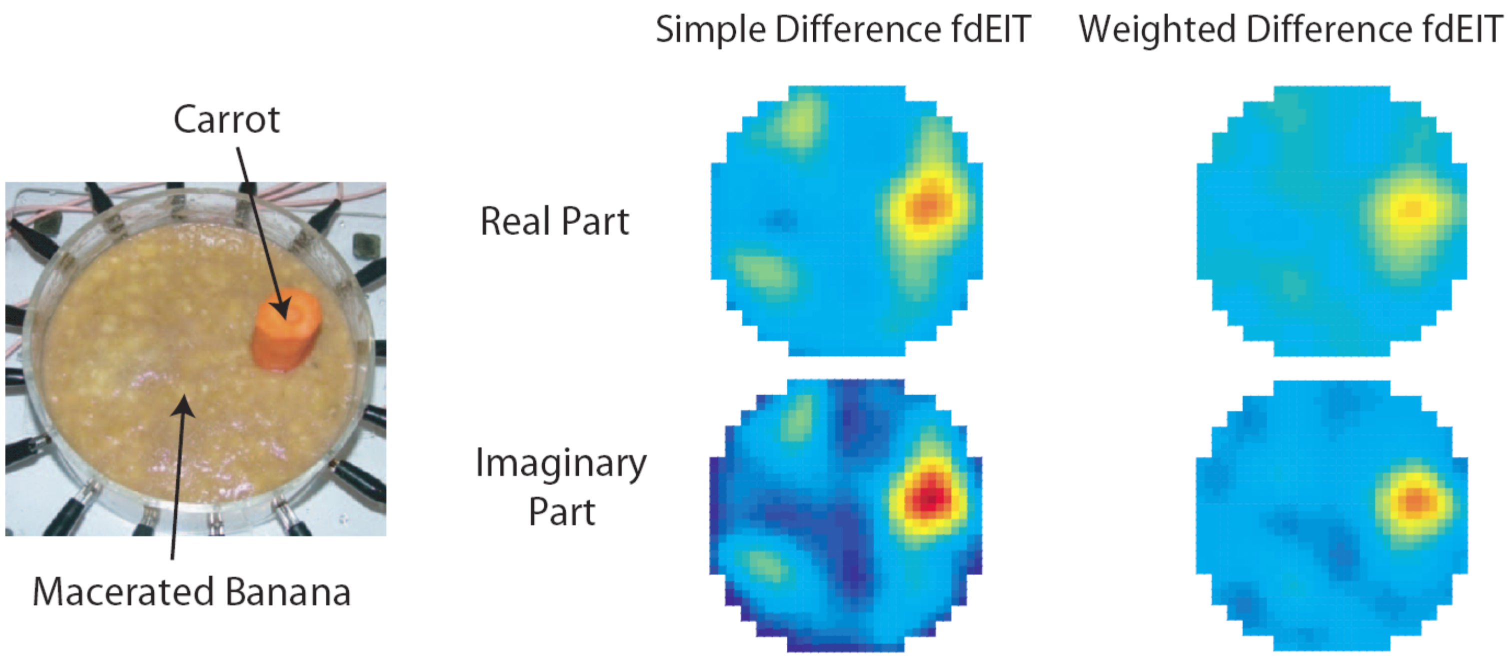

Imaging experiments using a homogeneous phantom including an anomaly of carrot in a background of macerated banana. The amounts artifacts are bigger in images using the simple difference.

Numerical simulation - 3D

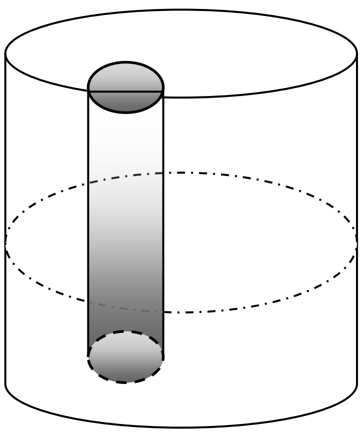

one-layer cylinder model

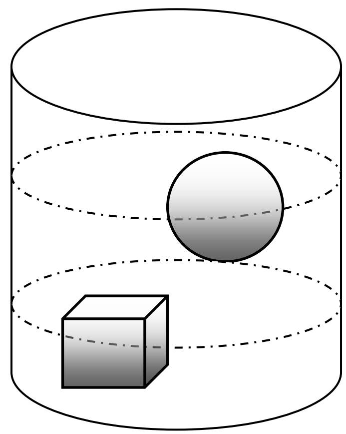

two-layer cylinder model

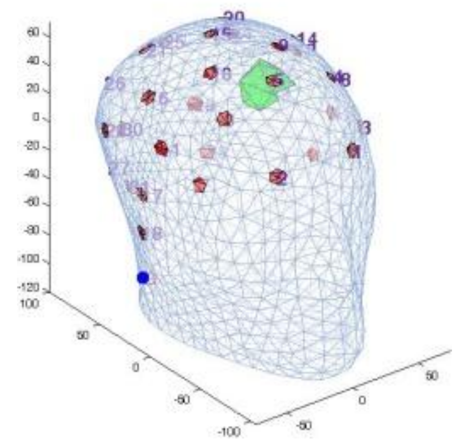

head model

Numerical simulation – one layer model

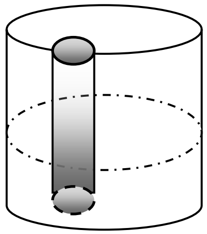

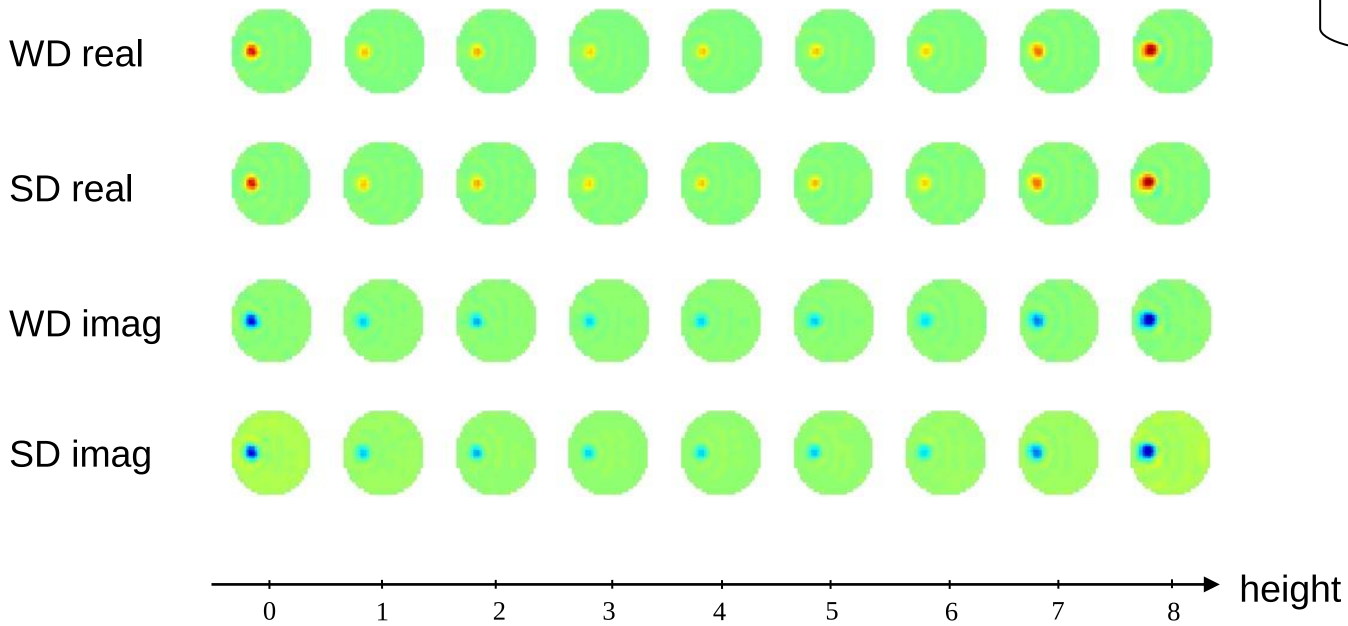

One-layer model filled with saline background and one cucumber anomaly

Numerical simulation – one layer model

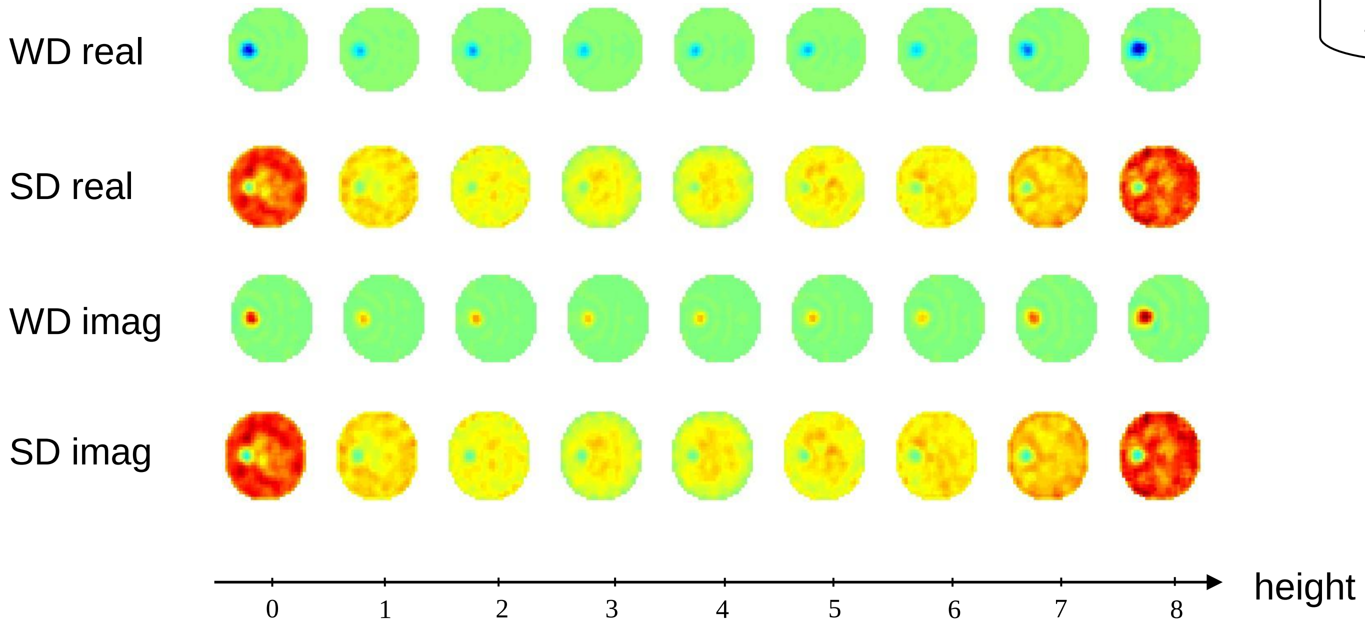

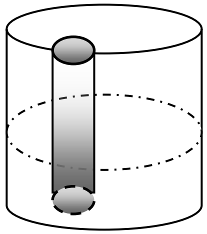

One-layer model filled with banana background and one cucumber anomaly

Numerical simulation – two layer model

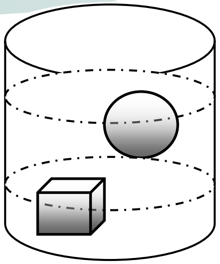

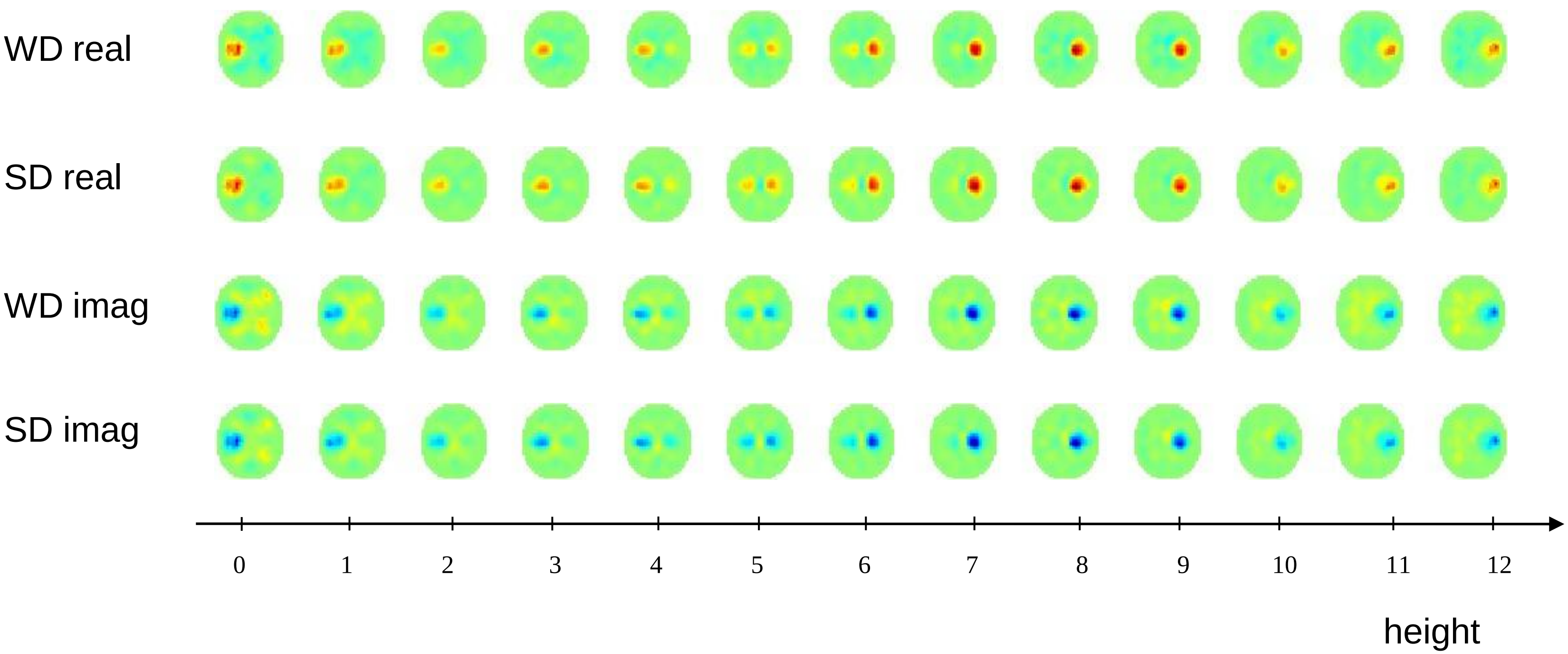

Two-layer model filled with saline background and one cucumber anomaly

Numerical simulation – two layer model

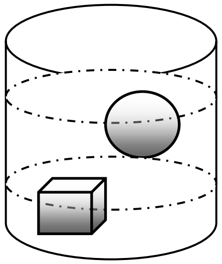

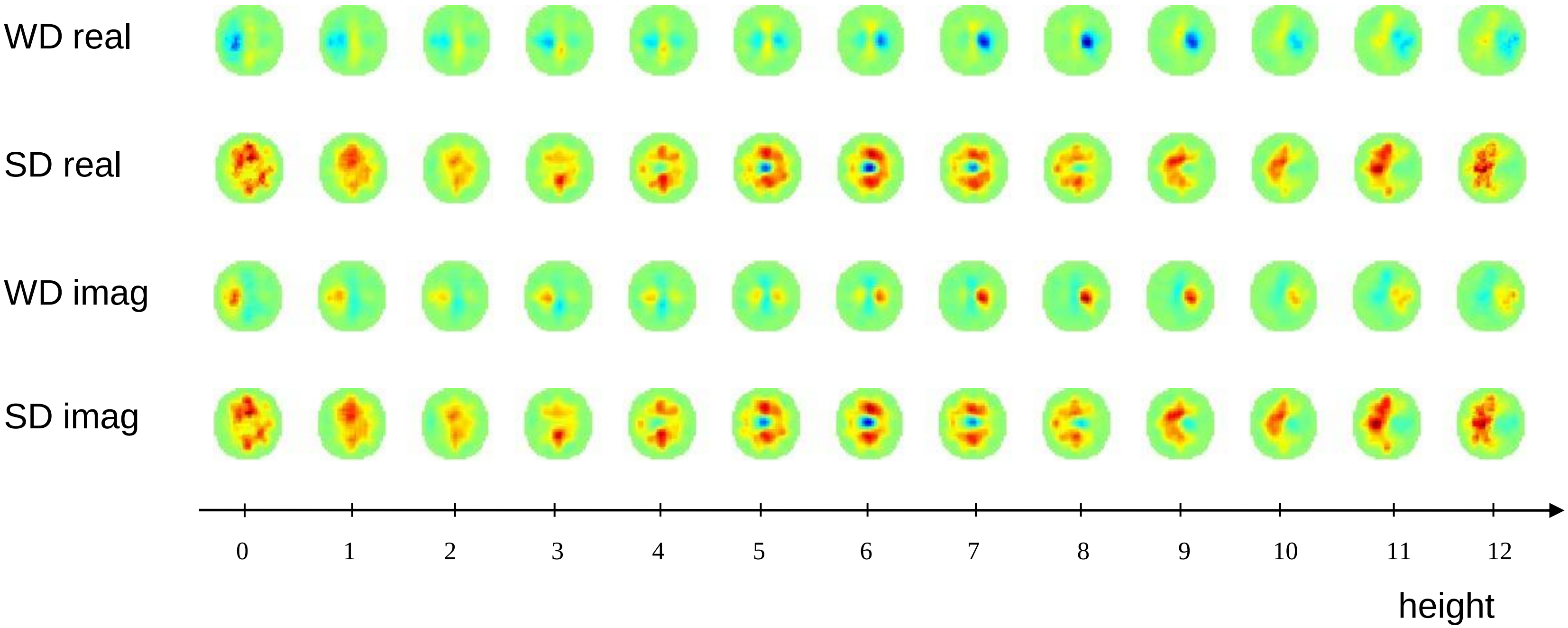

Two-layer model filled with banana background and one cucumber anomaly

Numerical simulation – realistic head model

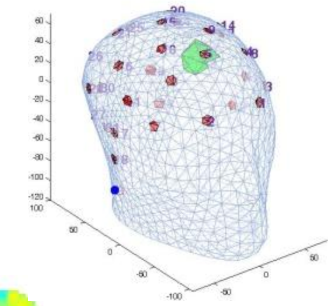

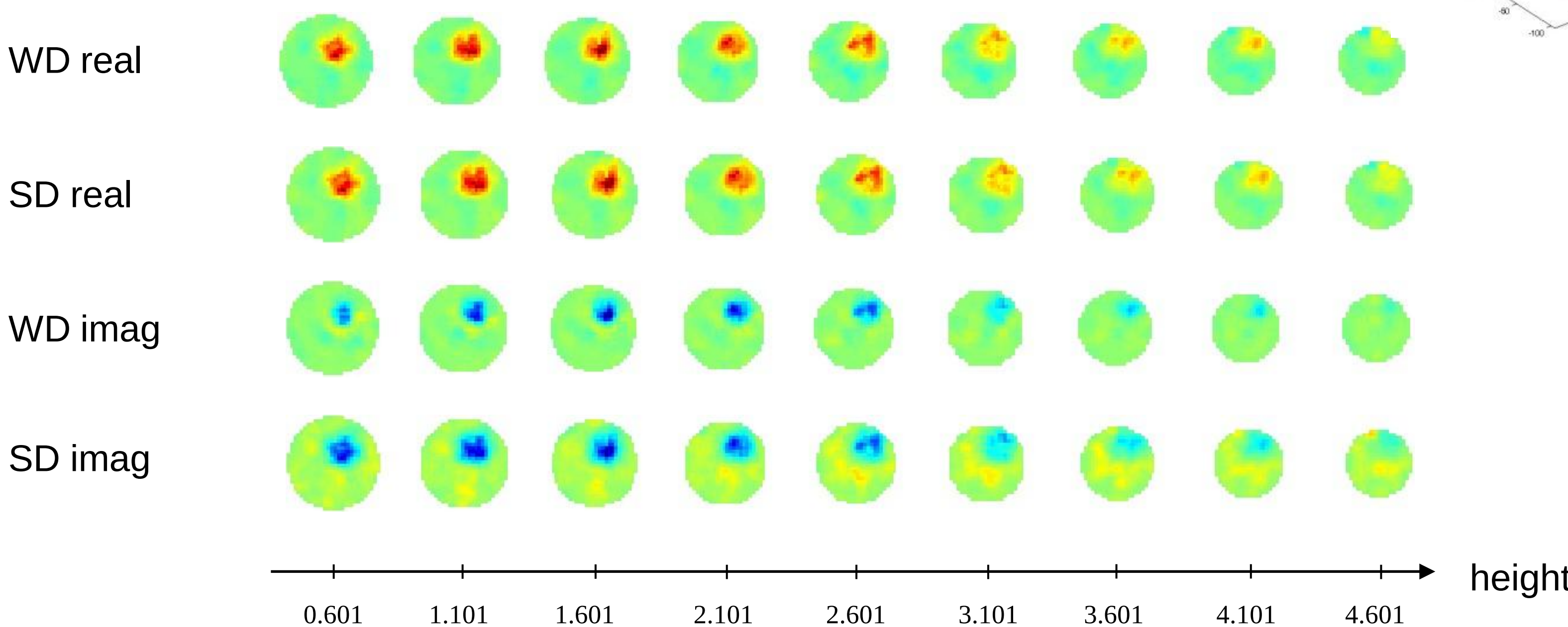

head model filled with saline background and one cucumber anomaly

Numerical simulation – realistic head model

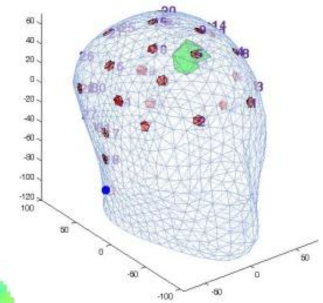

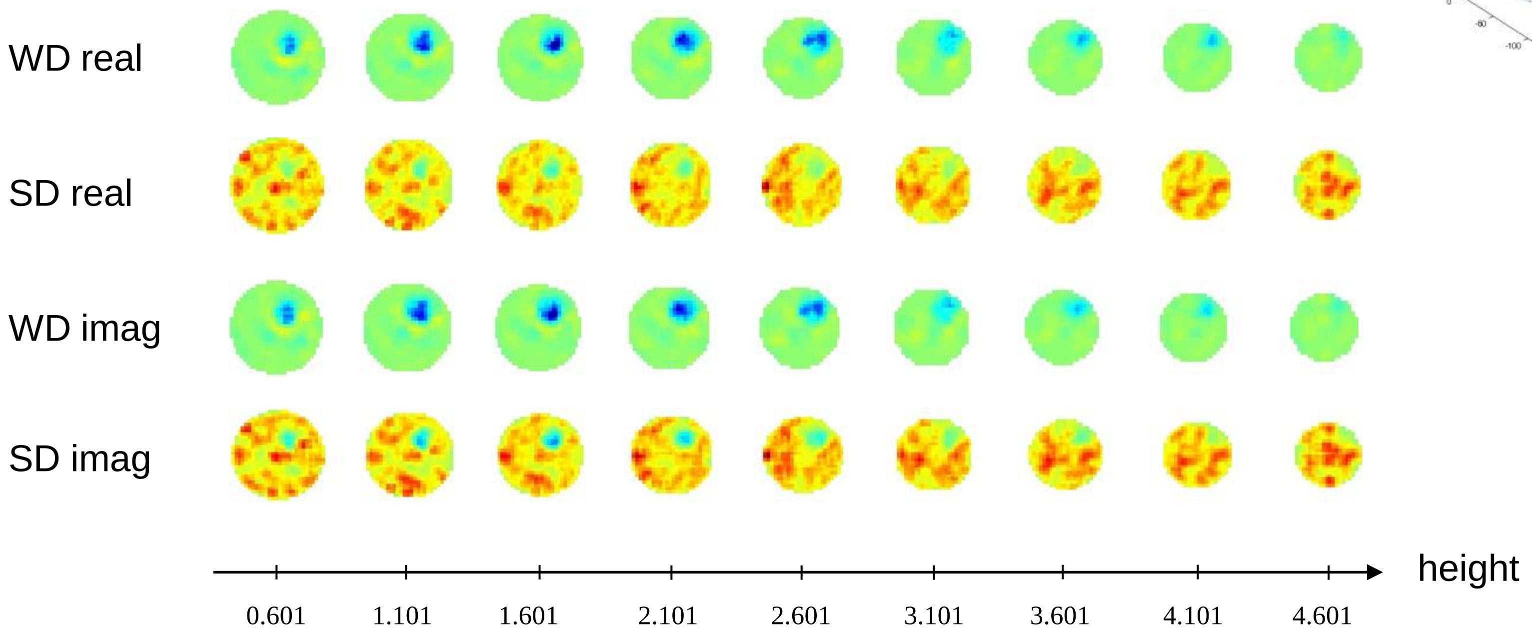

head model filled with banana background and one cucumber anomaly

Thank You !